

Hydraulic Capacity of an ADA Compliant Street Drain Grate

**Transportation Research and Analysis Computing Center
Energy Systems Division**

About Argonne National Laboratory

Argonne is a U.S. Department of Energy laboratory managed by UChicago Argonne, LLC under contract DE-AC02-06CH11357. The Laboratory's main facility is outside Chicago, at 9700 South Cass Avenue, Argonne, Illinois 60439. For information about Argonne and its pioneering science and technology programs, see www.anl.gov.

DOCUMENT AVAILABILITY

Online Access: U.S. Department of Energy (DOE) reports produced after 1991 and a growing number of pre-1991 documents are available free via DOE's SciTech Connect (<http://www.osti.gov/scitech/>)

Reports not in digital format may be purchased by the public from the National Technical Information Service (NTIS):

U.S. Department of Commerce
National Technical Information Service
5301 Shawnee Rd
Alexandria, VA 22312
www.ntis.gov
Phone: (800) 553-NTIS (6847) or (703) 605-6000
Fax: (703) 605-6900
Email: orders@ntis.gov

Reports not in digital format are available to DOE and DOE contractors from the Office of Scientific and Technical Information (OSTI):

U.S. Department of Energy
Office of Scientific and Technical Information
P.O. Box 62
Oak Ridge, TN 37831-0062
www.osti.gov
Phone: (865) 576-8401
Fax: (865) 576-5728
Email: reports@osti.gov

Disclaimer

This report was prepared as an account of work sponsored by an agency of the United States Government. Neither the United States Government nor any agency thereof, nor UChicago Argonne, LLC, nor any of their employees or officers, makes any warranty, express or implied, or assumes any legal liability or responsibility for the accuracy, completeness, or usefulness of any information, apparatus, product, or process disclosed, or represents that its use would not infringe privately owned rights. Reference herein to any specific commercial product, process, or service by trade name, trademark, manufacturer, or otherwise, does not necessarily constitute or imply its endorsement, recommendation, or favoring by the United States Government or any agency thereof. The views and opinions of document authors expressed herein do not necessarily state or reflect those of the United States Government or any agency thereof, Argonne National Laboratory, or UChicago Argonne, LLC.

Hydraulic Capacity of an ADA Compliant Street Drain Grate

prepared by
S.A. Lottes and C. Bojanowski
Transportation Research and Analysis Computing Center (TRACC)
Energy Systems Division, Argonne National Laboratory

September 2015

Acknowledgements

The authors would like to thank Andrea Herdrickson, Lisa Sayler, and Alan Rindels of the Minnesota Department of Transportation for providing test conditions, guidance, and their support of the project.

The work was performed at Argonne National Laboratory, managed and operated by UChicago Argonne, LLC, for the U.S. Department of Energy under Contract No. DE-AC02-06CH11357. The project was funded under an Interagency Agreement with the U.S. Department of Transportation through the Turner-Fairbank Highway Research Center, using the Federal Highway Administration Transportation Pooled Fund TPF-5(279).

Table of Contents

Chapter 1 Introduction and Background	1
Chapter 2 Grate Geometries and Test Cases	2
2.1 ADA Compliant Grate and Vane Grate for Comparison of Hydraulic Performance	2
2.2 Case Set Used for Performance Analysis	2
2.3 Determination of Water Flow Rate	4
2.4 Street, Gutter, and Curb Roughness for CFD Analysis	5
Chapter 3 CFD Model Construction	7
3.1 Geometry of CFD Model and Boundary Conditions	7
3.2 Design of the Computational Mesh	9
Chapter 4 Results and Discussion of ADA Complaint versus Vane Grate Performance	13
4.1 3D CFD Results	13
4.2 Tabulated Case Results	16
4.3 Effects of Increasing Longitudinal Street Slope	18
4.4 Correlation of All Case Results with Upstream Reynolds Number and Froude Number at Curb.....	24
Chapter 5 Summary and Conclusions	29

List of Figures

Figure 2.1 ADA compliant grate	2
Figure 2.2 Vane grate.....	2
Figure 2.3 Cross street geometry with single gutter and street cross slope	4
Figure 2.4 Composite cross street geometry	5
Figure 3.1 CFD approach to determining grate performance	8
Figure 3.2 Typical extent of the domain in CFD models	8
Figure 3.3 Volume mesh: cut through upstream grate slot showing cell density on left, fine mesh of polyhedral cell faces at street interface on grate surface with increasing size into catch basin on right.....	10
Figure 3.4 Parts based meshing with mixed mesh types improves accuracy. (1) catch basin including grate (2) region immediately over the grate (3) street with air above.	11
Figure 3.5 Polys in grate region minimize numerical diffusion	11
Figure 3.6 Extended domain test with coarser grid shows smaller domain is O.K. (and less expensive to run).....	12
Figure 4.1 Bypass flow at curb flows back into grate for low velocity case	13
Figure 4.2 Water surface for ADA compliant grate case 10 showing relatively high water depth over the entire grate	14
Figure 4.3 Water surface for ADA compliant grate case 8 showing only a small portion of the downstream end of the grate not covered by the water surface	15
Figure 4.4 Water surface vane grate case 10.1 showing large part of downstream portion of the grate not covered by water surface	15
Figure 4.5 Fraction of total flow captured by ADA compliant grate for three sets of cross street conditions	20
Figure 4.6 Fraction of total flow captured by vane grate for three sets of cross street conditions	20
Figure 4.7 Comparison for flow captured by ADA and vane grate showing more rapid drop off in performance of ADA grate as longitudinal street slope increases with 8 ft. spread	21
Figure 4.8 Comparison for flow captured by ADA and vane grate showing more rapid drop off in performance of ADA grate as longitudinal street slope increases with 10 ft. spread	21
Figure 4.9 Comparison for flow captured by ADA and vane grate showing more rapid drop off in performance of ADA grate as longitudinal street slope increases with 8 ft. spread and 0.02 street cross slope	22
Figure 4.10 Comparison of flow entering over ADA and vane grate from side showing more rapid drop off in performance of ADA grate with 8 ft. spread	23
Figure 4.11 Comparison of flow entering over ADA and vane grate from side showing more rapid drop off in performance of ADA grate with 10 ft. spread	23
Figure 4.12 Comparison of flow entering over ADA and vane grate from side showing more rapid drop off in performance of ADA grate with 8 ft. spread and 0.02 gutter cross slope .	24

Figure 4.13 Fraction of flow captured by grates correlated with upstream Reynolds number.....	26
Figure 4.14 Fraction of flow over grate from the side correlated with upstream Froude number at the curb water depth.....	27
Figure 4.15 Fraction of flow directly over that grate that is captured by the grate correlated with upstream Reynolds number.....	28

List of Tables

Table 2.1 Cases 3

Table 4.1 ADA compliant case results 16

Table 4.2 Vane grate case results..... 17

Executive Summary

Resurfacing of urban roads with concurrent repairs and replacement of sections of curb and sidewalk may require pedestrian ramps that are compliant with the American Disabilities Act (ADA), and when street drains are in close proximity to the walkway ADA compliant street grates may also be required. The Minnesota Department of Transportation (MnDOT) ADA Operations Unit identified a foundry with an available grate that meets ADA requirements, but no information on the hydraulic capacity of the grate for on-grade conditions was available. Flume testing of street grates is very expensive, difficult to schedule, and cannot be done easily under full scale street conditions. Argonne National Laboratory's Transportation Research and Analysis Computing Center (TRACC) used full scale three dimensional computational fluid dynamics (CFD) software to determine the hydraulic performance of the ADA compliant grate and compared it to the performance of the standard vane grate specified by MnDOT. The project was funded under an Interagency Agreement with the Turner-Fairbank Highway Research Center (TFHRC), using FHWA pooled fund TPF-5(279).

The ADA compliant grate geometry was R-3210-Q from the Neenah grate catalog and the vane grate geometry was R-3210-L from the Neenah grate catalog. A parametric set of test cases was specified by MnDOT. These included street geometry with 0.04 gutter cross slope, 0.02 and 0.04 street cross slopes for six street longitudinal slopes ranging from 0.003 to 0.06. A few additional cases with varied gutter cross slopes were run with a street longitudinal slope of 0.01. Water spreads across the street were 8 and 10 feet including a 2 foot gutter width.

The CFD model used a volume of fluid model (VOF) that is routinely used for computation of free surface flows of immiscible fluids in this case water and air. The domain was divided into three regions to allow generation of near optimum computational meshes in each region. The regions were: (1) a 20 foot long by 10 foot wide section of street with water and air above it, (2) the volume immediately above the grate, and (3) the grate and catch basin section cut at about 1.5 feet below the street level.

The ADA compliant grate has a large number of much narrower slots than those used in the common street drain grates, and therefore its hydraulic performance was expected to be below that of the vane grate. The hydraulic performance of the grates was characterized by the fraction of the total volume flow approaching the longitudinal position of the grate from the upstream that was captured by the grate and diverted into the catch basin. The fraction of the total flow entering over the grate from the side and the fraction of flow directly over a grate that is diverted into the catch basin were also result quantities of interest that aid in understanding the differences in performance of the grates in the study.

As expected, the performance of the ADA compliant grate was lower than that of the vane grate in each of the test cases. As the volume flow rate is reduced below those of the test cases, there is

a volume flow low enough, which was not determined, where the ADA grate would capture all of the flow making the performance of the two grates equal for conditions with volume flows less than that amount. The lowest volume flow rate tested was 0.867 cfs with a gutter cross slope of 0.04, a street cross slope of 0.02, an 8 foot water spread, and street longitudinal slope of 0.003. For these conditions, the performance of the ADA compliant and vane grate were very close, within 3% of each other, with the vane grate capturing 77% of the total flow and the ADA compliant grate capturing 75%. The largest difference in performance occurred at the highest volume flow rate of 19.6 cfs with a gutter and street cross slope of 0.04, a 10 foot water spread, and a longitudinal slope of 0.06. For these conditions, the vane grate performance was three times that of the ADA compliant grate. The vane grate captured 38% of the total flow while the ADA compliant grate captured only 13%.

Three sets of cases were tested where only the longitudinal street slope parameter was varied from 0.003 to 0.06. In these case sets the water volume flow rate and mean velocity increases with increasing longitudinal street slope. For these case sets, the performance of the two grate types was relatively close at the lowest longitudinal street slope and corresponding low volume flow rate. In the worst case set, the ADA compliant grate performance was about 12% below that of the vane grate. As the longitudinal street slope was increased, the performance of both grates decreased, but the performance of the ADA compliant grate decreased much faster than the vane grate, yielding in the worst case, a vane grate hydraulic performance that was 3 times the ADA compliant grate performance.

Single parameter correlations were sought to characterize the relation between the various parameters and grate performance quantified as the fraction of total flow captured by the grate. Relations were also sought for the fraction of total flow entering over the grate from the side of the grate and the fraction of the flow directly over the grate that is captured by the grate. The upstream Reynolds number, defined in terms of the water volume flow rate and curb and street wetted perimeter was found to be the best parameter to correlate with the fraction of total flow captured by the grates and with the fraction of flow directly over the grate that is captured by the grate. The upstream Reynolds number represents a ratio of flow inertia to the viscous resistance of the flow by the street and curb surfaces. The relation between Reynolds number and grate performance was found to be best fit for all cases by a logarithmic decay function of the form $C_f = -A \ln(R_e) + B$, where A and B are fitting constants and C_f is the fraction of flow captured by the grate. The coefficient of determination of these relations was 0.90 for the vane grate cases and 0.94 for the ADA compliant grate cases, indicating a very high degree of correlation between upstream Reynolds number and grate performance under varying street geometry and flow conditions. For the ADA compliant grate, that pre-logarithm constant was 0.215, nearly twice that for the vane grate with $A = 0.125$. For upstream Reynolds numbers less than about 120,000 the flow captured by the grates is comparable, with the ADA compliant grate capturing 90% or more of the flow fraction captured by the vane grate. However, as Reynolds number increases, the performance of the ADA grate drops logarithmically. At Reynolds number 200,000 the ADA grate performance

is about 25% lower than the vane grate and at 600,000 the ADA compliant grate captures half the flow captured by the vane grate.

The major factor leading to the hydraulic performance difference between the two grates appears to be the fraction of flow directly over the grates that is captured by the grates. The difference is clearly seen when this quantity is plotted against upstream Reynolds number. Nearly all of the flow entering into the space directly above the vane grate is captured and diverted into the catch basin. A drop off of only 3% occurs from Reynolds number 50,000 to 800,000. For the ADA compliant grate, the fraction of flow directly over the grate drops linearly from 100% at Reynolds number 50,000 to only 34% at a Reynolds number of about 790,000.

Chapter 1

Introduction and Background

When urban roads are resurfaced with concurrent repair and/or replacement of sections of curb and sidewalks, Americans with Disabilities Act (ADA) compliant pedestrian ramps at crosswalks may be required. Storm drains are often located near crosswalks, and may be in the crosswalk. In that case, an ADA compliant replacement grate would be required. The Minnesota Department of Transportation (MnDOT) ADA Operations Unit identified a foundry with an available grate that meets ADA requirements, but no information on the hydraulic capacity of the grate for on-grade conditions was available.

The openings in ADA compliant grates are smaller than traditional grates and their hydraulic capacity is less. In order to maintain total street drainage capacity when ADA compliant grates are used, the hydraulic capacity of ADA compliant designs must be determined. Computational Fluid Dynamics (CFD) analysis was used as an alternative to flume testing of the identified ADA compliant grate. Traditionally flume testing of grate capacity is done, however, flume conditions do not correspond directly to street conditions, and therefore procedures are needed to calculate capacities under full scale street design conditions. In addition, flume testing may require modification of a flume at a Federal Highway Administration (FHWA) laboratory or university flume and scheduling of time to run tests at that facility. CFD analysis of grates can be carried out at full scale for a variety of street slopes and water volume flow rates by modifying the model geometry.

Argonne National Laboratory's Transportation Research and Analysis Computing Center (TRACC) has been conducting CFD analysis of hydraulic problems for and in collaboration with the Turner-Fairbank Highway Research Center (TFHRC) since 2007. TRACC analysts conducted a brief feasibility study and determined that grate hydraulic capacity could be determined using CFD. This report covers the analysis of an ADA compliant grate in comparison to a traditional vane grate specified by MnDOT to determine hydraulic performance under a matrix of full scale street conditions specified by MnDOT. The study was funded by MnDOT through the Federal Highway Administration (FHWA) Transportation Focused Fund Program study number TPF-5(279).

Chapter 2

Grate Geometries and Test Cases

2.1 ADA Compliant Grate and Vane Grate for Comparison of Hydraulic Performance

The ADA compliant grate geometry is R-3210-Q from the Neenah grate catalog as shown in Figure 2.1 [1]. These grates consist of fourteen rows by four columns of slots. The slot openings are one half inch by four and one half inches. The rows are spaced one inch apart, and the columns are spaced one and one eighth inch apart. The top of the grate is 22 inches by 22 inches.

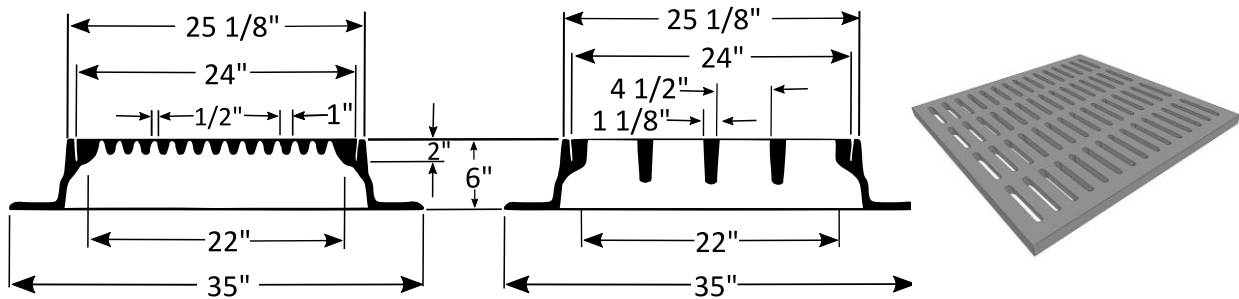


Figure 2.1 ADA compliant grate

The grate modeled for comparison with the ADA compliant grate was a grate with five rows of holes separated by guide vanes referred to in this report as the “vane grate.” This grate is the R-3210-L grate in the Neenah grate catalog as shown in Figure 2.2 [1]. It consists of five rows of seven holes. The holes are two and five eighths inches wide, and the guide vanes are spaced at four and one quarter inches from tip to tip. The vanes have a curved cross section that varies in thickness with curvature, but are approximately one inch.

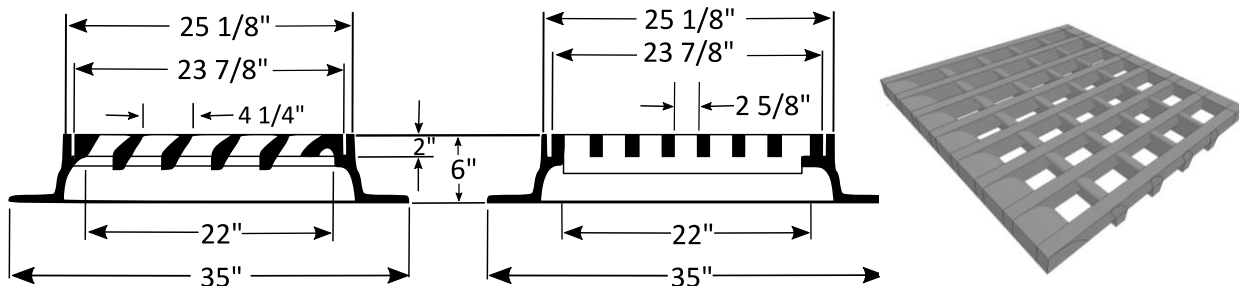


Figure 2.2 Vane grate

2.2 Case Set Used for Performance Analysis

The set of cases analyzed to determine grate hydraulic performance was specified by MnDOT and included the statement of work for the project. The cases are listed in Table 2.1. The cases in the table with integer numbers are the original cases specified by MnDOT. A few additional cases, numbered with a “dot 1” following the integer case number are extra cases that

were run to verify trends in the results. The gutter width for all cases is two feet. The cases have pavement widths of 6 and 8 feet. Subsets of cases with varying street longitudinal slope have a gutter cross slope of 0.04, with pavement cross slopes of 0.02 and 0.04. The wetted pavement widths analyzed were 6 and 8 feet. The longitudinal slopes were 0.003, 0.005, 0.01, 0.03, 0.05, and 0.06. Additional cases with gutter cross slopes of 0.02 and 0.05 were analyzed using a street longitudinal slope of 0.01.

Table 2.1 Cases

Case	Cross Street Slope Type	Gutter Cross Slope (S _w)	Street Cross Slope (S _x)	Street Longitudinal Slope (S _L)	Wet Pavement Width (P _s) (ft)	Water Depth at Curb (ft)	Vol. Flow (Q) (cfs)	Inlet Vel. Ave. (ft/s)	Inlet Curb Froude No. (Fr)	Inlet Reynolds No. (Re)
1	Single	0.04	0.04	0.003	6	0.32	2.42	1.89	0.59	121 300
2	Single	0.04	0.04	0.005	6	0.32	3.12	2.44	0.76	156 600
3	Single	0.04	0.04	0.01	6	0.32	4.42	3.46	1.08	221 500
4	Single	0.04	0.04	0.03	6	0.32	7.65	5.99	1.87	383 600
5	Single	0.04	0.04	0.05	6	0.32	9.88	7.73	2.41	495 200
5.1	Single	0.04	0.04	0.06	6	0.32	10.82	8.47	2.64	542 500
6	Single	0.04	0.04	0.003	8	0.40	4.39	2.20	0.61	176 100
7	Single	0.04	0.04	0.005	8	0.40	5.67	2.84	0.79	227 300
8	Single	0.04	0.04	0.01	8	0.40	8.01	4.01	1.12	321 500
9	Single	0.04	0.04	0.03	8	0.40	13.88	6.95	1.94	556 800
10	Single	0.04	0.04	0.05	8	0.40	17.92	8.98	2.50	718 800
10.1	Single	0.04	0.04	0.06	8	0.40	19.63	9.83	2.74	787 400
11	Comp	0.04	0.02	0.003	6	0.20	0.87	1.28	0.50	44 100
12	Comp	0.04	0.02	0.005	6	0.20	1.12	1.65	0.65	56 900
13	Comp	0.04	0.02	0.01	6	0.20	1.58	2.33	0.92	80 500
14	Comp	0.04	0.02	0.03	6	0.20	2.74	4.04	1.59	139 500
14.1	Comp	0.04	0.02	0.04	6	0.20	3.17	4.66	1.84	161 100
15	Comp	0.04	0.02	0.05	6	0.20	3.54	5.21	2.05	180 100
15.1	Comp	0.04	0.02	0.06	6	0.20	3.88	5.71	2.25	197 200
16	Comp	0.02	0.04	0.01	8	0.36	7.68	3.93	1.15	309 400
17	Comp	0.02	0.04	0.01	6	0.28	4.14	3.34	1.11	208 400
18	Single	0.02	0.02	0.01	6	0.16	1.39	2.17	0.96	71 100
19	Comp	0.05	0.04	0.01	8	0.42	8.19	4.06	1.10	327 700
20	Comp	0.05	0.04	0.01	6	0.34	4.56	3.52	1.06	228 200
21	Comp	0.05	0.02	0.01	6	0.22	1.69	2.41	0.91	85 600

The case table lists type of cross street slope geometry as single when the gutter cross slope and street cross slope are equal and as composite (Comp) when they are not equal. The Urban

Drainage Design Manual, HEC 22, was used to calculate the volume flow rate, Q , based on the street geometry and the wetted width of the street [2].

2.3 Determination of Water Flow Rate

For streets with a single cross street and gutter slope, the geometry is shown in Figure 2.3, and the HEC 22 formula for the volume flow rate, Q , is:

$$Q = \left(\frac{K_u}{n} \right) S_x^{1.67} S_L^{0.5} T^{2.67} \quad 2.1$$

where $K_u = 0.56$ for English units (0.376 for metric units), n is Manning's coefficient, T is the width of the water surface covering the gutter and street, S_x is the gutter and street cross slope, and S_L is the longitudinal slope.

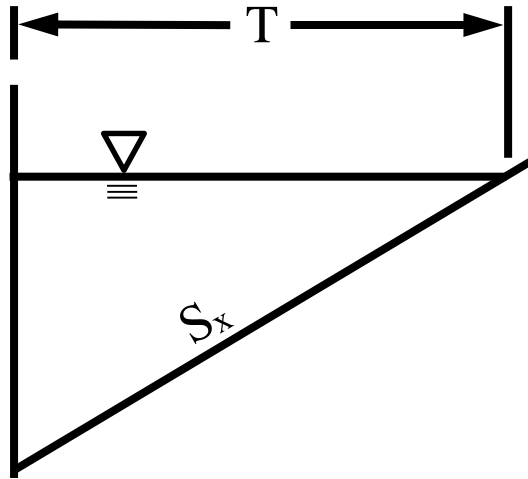


Figure 2.3 Cross street geometry with single gutter and street cross slope

The composite cross street geometry with different gutter and street cross slopes is shown in the diagram in Figure 2.4, and the HEC 22 formula for volume flow rate, Q , for this geometry is:

$$Q = Q_s / (1 - E_0) \quad 2.2$$

where Q_s is the flow capacity of the section above the depressed section, E_0 is the ratio of flow in wet width of street to the total section flow, $E_0 = Q_w / Q$, $Q = Q_s + Q_w$, and $S_w = S_x + a/W$.

$$E_0 = \left(1 + \frac{\frac{S_w}{S_x}}{\left(\frac{1 + \frac{S_w}{S_x}}{\frac{T}{W^{-1}}} \right)^{2.67} - 1} \right)^{-1}$$

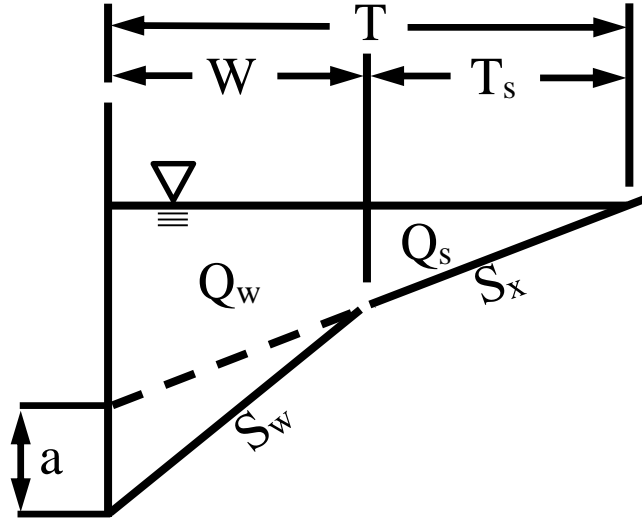


Figure 2.4 Composite cross street geometry

Equations 2.1 through 2.3 were programmed in a Python program to compute the volume flow rate for the set of cases in Table 2.1. The program was checked against the example cases for simple and cross street geometry given in HEC 22 to verify that the computed flow rates matched [2].

2.4 Street, Gutter, and Curb Roughness for CFD Analysis

The Manning n value of roughness for pavement, gutter, and curb specified by MnDOT for the grate analysis was 0.015. The CFD software does not accept a Manning n value to set surface resistance due to roughness; instead, the equivalent roughness parameter, k_s , in the Colebrook-White equation is required to set surface roughness [3]. The conversion of a Manning n value to an equivalent roughness, k_s , is discussed in McGahey and Samuels, 2004 [4]. They cite the work of Strickler, 1923, and Ackers, 1958, to obtain the following conversion formula:

$$n = 0.038 k_s^{\frac{1}{6}} \quad 2.4$$

This equation is only considered to be applicable when the water depth, h , is in the range of 7 to 140 times the roughness size.

The Colebrook-White equation for fully rough turbulent flow is

$$\frac{1}{\sqrt{f}} = -2.03 \log \frac{k_s}{12.27h} \quad 2.5$$

where the friction factor f is related to the Manning n parameter by

$$f = \frac{8gn^2}{h^{\frac{1}{3}}} \quad 2.6$$

where g is the gravity constant. Combining equations 2.5 and 2.6 yields

$$k_s = 12.27 h 10^{\left[\frac{h^{\frac{1}{6}}}{-2.03 n \sqrt{8g}} \right]} \quad 2.7$$

For a depth of 4.8 in. (0.12 m), the roughness value, k_s , calculated from Ackers formula (Eq. 2.4) is 3.8 mm, and the k_s value calculated using Eq. 2.7 is 3.7 mm. These values appear reasonable for asphalt and close enough for engineering computations. As noted in McGahey and Samuels, 2004, the values of k_s obtained from these formulas may differ by an order of magnitude or more when the depth and Manning n value are not close to those used here, and they propose that Equation 2.7 is preferred because k_s/h remains bounded as n becomes large [4].

Chapter 3

CFD Model Construction

3.1 Geometry of CFD Model and Boundary Conditions

The CFD model requires a domain that includes the street upstream and downstream of the grate, the water in the street, and space for air above the water so the height of the free surface can be computed with the solution. It also includes the grate and a portion of the catch basin below the grate that the water falls into when passing through the grate. Boundary conditions for all of the internal and external boundaries in the domain must be specified to solve the flow problem. A schematic of this domain with boundary condition types for the external boundaries is shown in Figure 3.1.

The symmetry plane condition for the vertical boundary near the center of the street affects only the air within the domain and could also be specified as a pressure boundary, but symmetry plane is likely more stable in this case. The upstream inlet for water and air at street level requires a velocity inlet. The velocity here is set to the mean velocity calculated as volume flow rate divided by cross section area, Q/A , where the water cross section is a triangle or composite polygon, when gutter and street cross slope are different, determined by the water depth at the curb and the width of water covered pavement. The remainder of the inlet area is the air above the water, and the air velocity is set slightly higher than the water velocity to reduce the formation of recirculation zones near exit boundaries for air, which has minimal impact on water flow due to the large viscosity difference, but does reduce warning messages.

Pressure boundary conditions are specified at the downstream exit plane at the street level and at the horizontal plane where water is dropping through to the bottom of the catch basin. The pressure boundary conditions at these water outlets allow fraction of water leaving the domain through the outlets to be computed as part of the solution of the flow in the system. The downstream outlet on the street is set to the value of the back pressure of water just beyond the outlet. This value is the static pressure minus the dynamic pressure due to flow. In the catch basin the water is in free fall, and the outlet pressure is set to atmospheric gauge pressure, which is zero. The top of the domain occupied by air is also set to a pressure boundary condition. This allows air to leave through the top boundary if the water level increases and air to enter through the top if the water level decreases.

All internal and external solid surfaces are set to be wall boundaries. The street, gutter, and curb roughness values were set to 0.15 inch (3.7 mm). Section 2.4 describes how this roughness value was obtained from the Manning value specified by MnDOT.

The domain schematic in Figure 3.1 is not drawn with the actual scale proportions in order to clearly label the boundaries. Figure 3.2 has the position of the grate in the domain with accurate proportions for one of the cases to illustrate the size and position of one of the grates with respect to the computational domain.

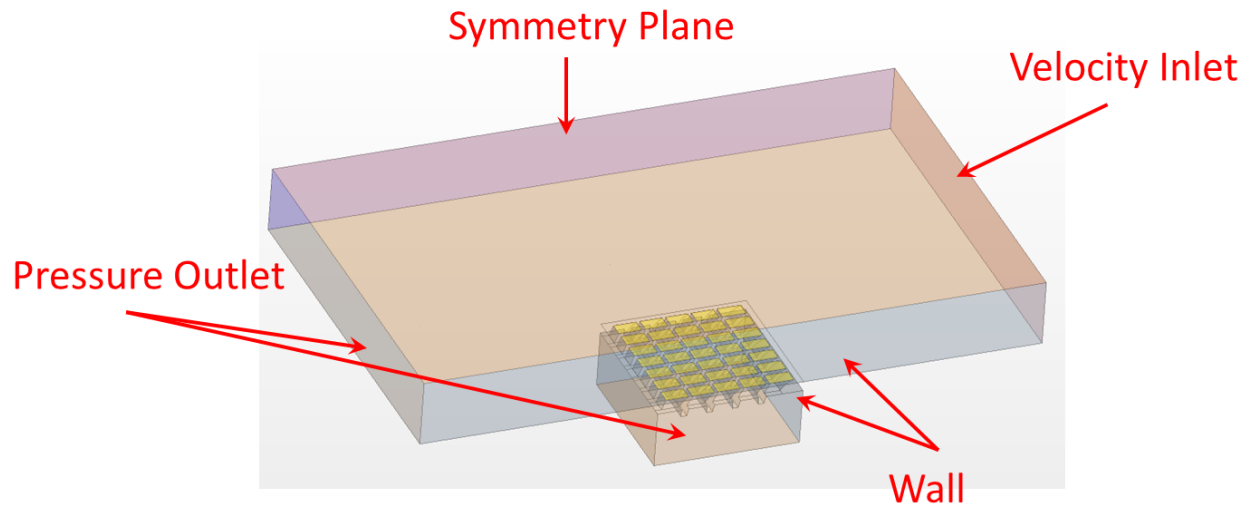


Figure 3.1 CFD approach to determining grate performance

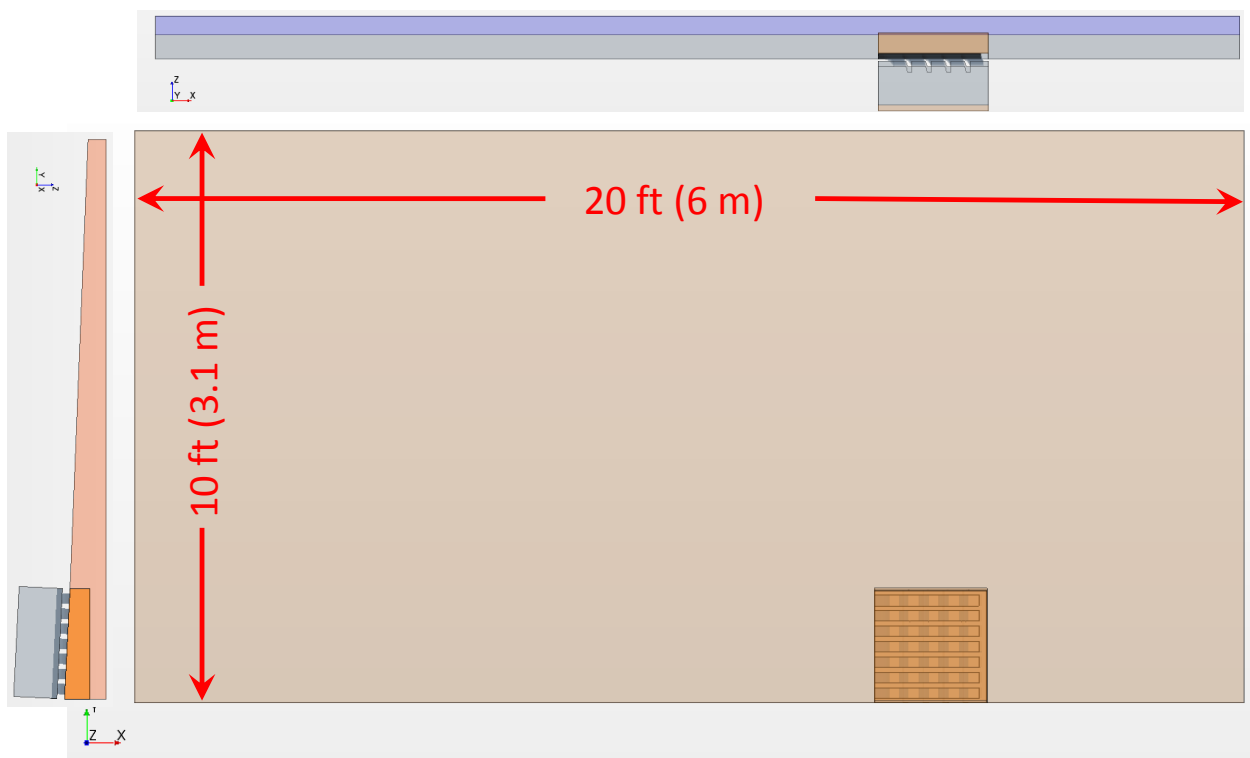


Figure 3.2 Typical extent of the domain in CFD models

3.2 Design of the Computational Mesh

A hexahedral mesh is used for all of the volume at and above the street, except for the space directly above the grate. Minimization of numerical diffusion occurs when the mesh cells are aligned to the extent possible with streamlines. A hexahedral mesh running parallel to the curb is in near alignment with water flow except over the grate where some or all of the flow turns down and flows into the grate.

Polyhedral mesh cells are best used to minimize numerical diffusion in regions where the flow turns, in this case over the grate and the part of the catch basin immediately below the grate entry. Polyhedral cells were used in these two zones for the computational mesh.

The domain was divided into three regions: (1) the upper section of the catch basin, (2) the volume immediately over the grate up to a height that exceeds the water depth for all of the cases to be run with a particular mesh, and (3) the volume containing water and air above the street excluding region 2, as shown in Figure 3.4. This division allows separate meshing with different mesh types in the regions. It also provides interfaces between regions that allow for integration of mass flow through the interface to determine the rate at which water flows through the grate into the catch basin, the rate at which water flows from the street over the grate from the front, from the side, and from the downstream side of the grate.

A more accurate calculation of flow captured by the grate is obtained by refining the mesh near the interface between the grate openings and the street level immediately above the grate. This is achieved by controlling the size of the surface mesh on the grate and grate hole interface. The target surface mesh size was set to 0.16 inch (4 mm) with a minimum surface size of 0.08 inch (2 mm). The target surface size at the bottom outlet of the model catch basin section was set to a much larger mesh size of 1.6 inch (4 cm) with a minimum surface size of 0.8 inch (2 cm). The volume mesh is generated by the mesher from the surface meshes, and consequently a very fine volume mesh is generated near the grate entry and it grows to much larger cell sizes in the direction of the bottom of the catch basin section. The total size of the computational mesh for all regions is about 7 million cells, a problem size that requires a high performance computing cluster to solve, and meshing with larger cells away from zones of interest keeps the mesh from becoming so large that it would require excessive computation time and resources to solve each case. With the 7 million cell mesh, the computation time on the TRACC Zephyr cluster is between 30 and 40 hours on 16 cores to reach a solution that is accurate in mass balance to nearly 3 significant figures.

Figure 3.3 shows typical volume mesh views of the polyhedral cells around the entry interface of an ADA compliant grate. The image on the left is a slice through the grate and region above near the upstream end of the grate, and the image on the right shows the polyhedral cell faces on the top surface of the grate at a corner including the sides of the catch basin.

Figure 3.4 shows a view of the portion of the mesh sliced through all three regions near the grate with the different cell types and refined mesh zone. It also shows the portion of the object tree in the user interface where the regions are defined. The water refinement block was created as one of the objects to create a finer hexahedral mesh in the lower street region where water is flowing. The zone above containing air can be coarser to save computation time and resources

because highly accurate computation of the air flow is not required, and the air flow has little effect on the water flow, except to provide a space for the water surface level to change.

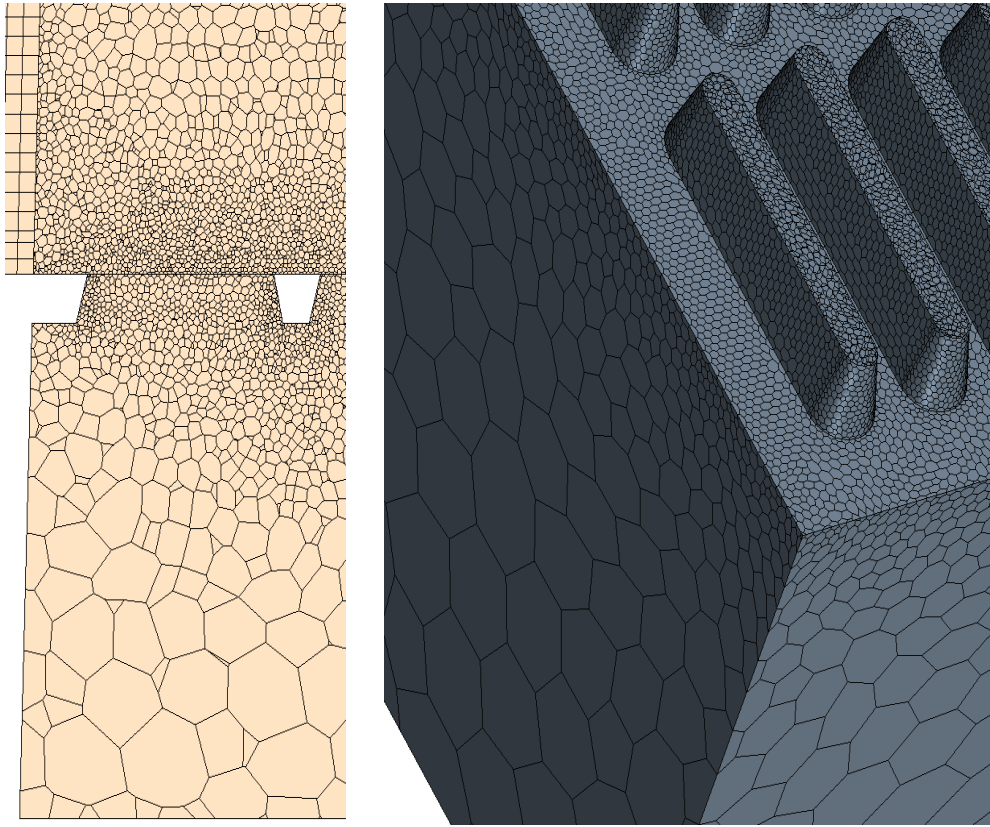


Figure 3.3 Volume mesh: cut through upstream grate slot showing cell density on left, fine mesh of polyhedral cell faces at street interface on grate surface with increasing size into catch basin on right.

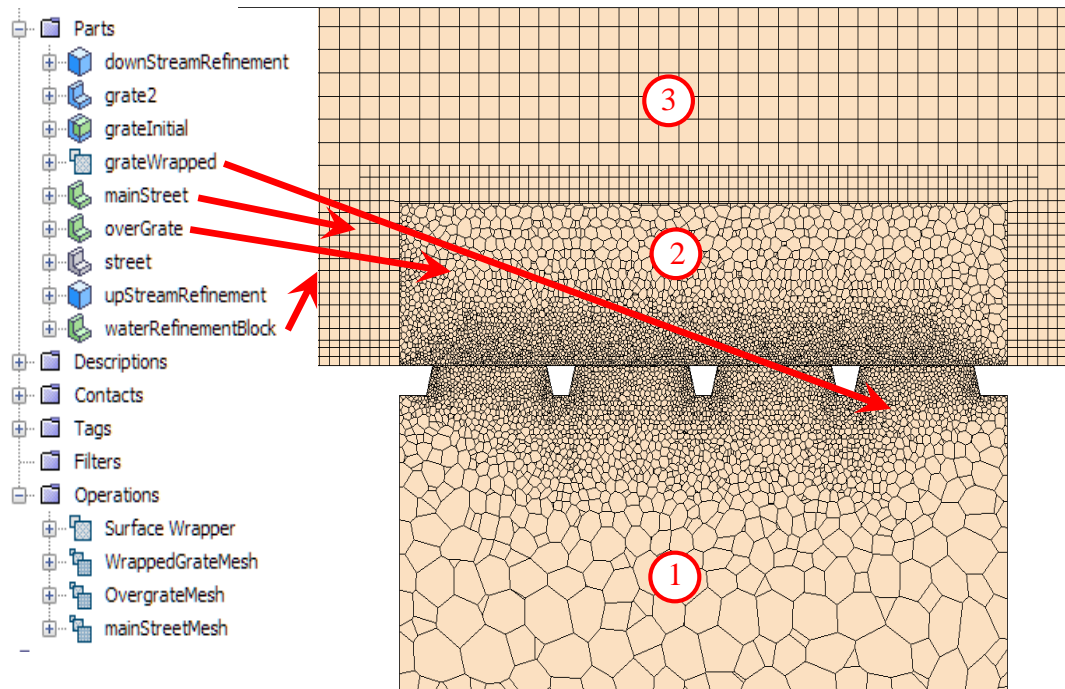


Figure 3.4 Parts based meshing with mixed mesh types improves accuracy. (1) catch basin including grate (2) region immediately over the grate (3) street with air above.

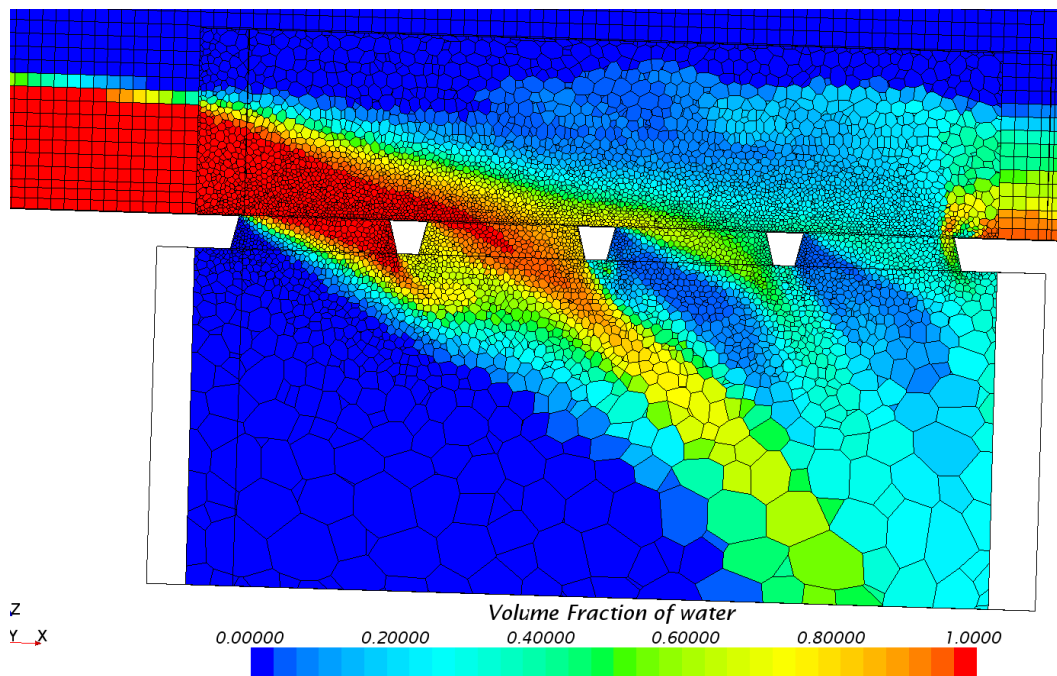


Figure 3.5 Polys in grate region minimize numerical diffusion

The outlet of the flow domain at street level must be placed far enough downstream so further changes of flow development in the downstream do not affect the upstream flow into the grate. Normally this is the case when the flow is nearly normal to the outlet with negligible gradients in the direction along the street. To verify that the outlet location was adequate, the size of the domain was doubled by extending the street twice the domain length into the downstream. A coarser grid was used for this test to allow the test to be completed within a couple of days. A case was then solved on this much longer domain and then compared to the results with the shorter designed domain. The doubled domain with plotted free surface is shown in Figure 3.6. No differences greater than approximately a fraction of a percent were noted, and therefore the design domain was judged adequate for running the case matrix.

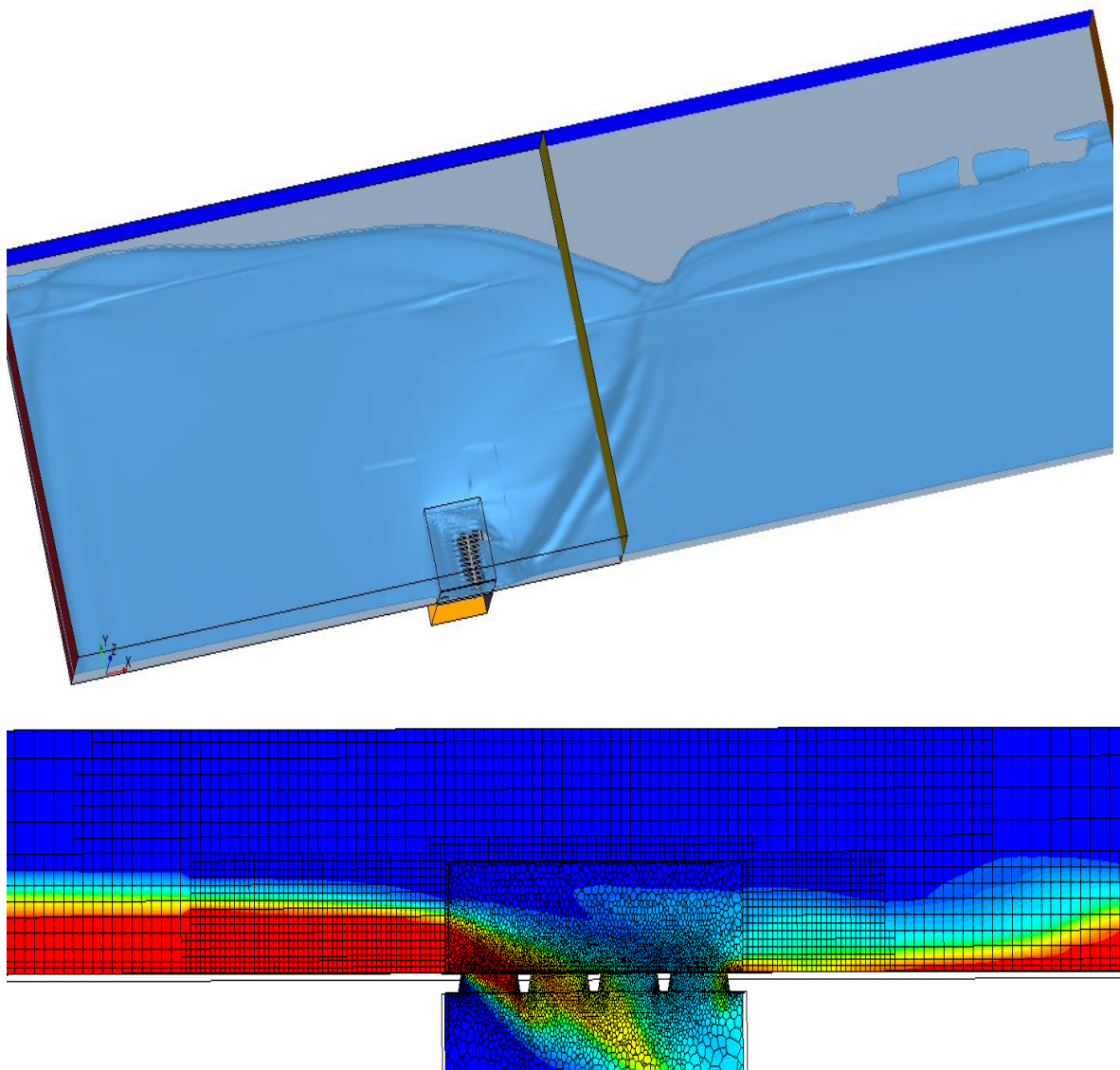


Figure 3.6 Extended domain test with coarser grid shows smaller domain is O.K. (and less expensive to run)

Chapter 4

Results and Discussion of ADA Complaint versus Vane Grate Performance

4.1 3D CFD Results

The visualization capabilities that are part of the CFD software package allow for a variety of scenes with the results of the analysis to be created that show what is happening in a way that is easy to understand. Several examples of such scenes were shown in the figures of Chapter 3 to illustrate aspects of the computational mesh design for the analysis. Three free surface visualizations of the flow past the grates are included here to illustrate features of the flow interaction with the grates that are related to the grate performance.

A low velocity ADA compliant grate case (11, Table 2.1) that illustrates backflow over the downstream end of the grate is shown in Figure 4.1. The water surface in blue has superimposed velocity vectors in black to show the direction of the flow. In this case the incoming velocity was 1.28 ft/s (0.389 m/s), which is low enough for flow coming from the upstream side to be completely captured by the grate and for bypass flow around the side of the grate to stagnate on the curb wall with some of the flow turning toward the upstream, entering over the grate at the downstream end, and flowing into the catch basin. For the ADA compliant grate this pattern only occurred for cases 11 and 12 in Table 2.1, which had an 8 foot water spread, 0.04 gutter cross slope and 0.02 street cross slope. Eight of the 25 vane grate cases had some back flow capture over the downstream end of the grate.

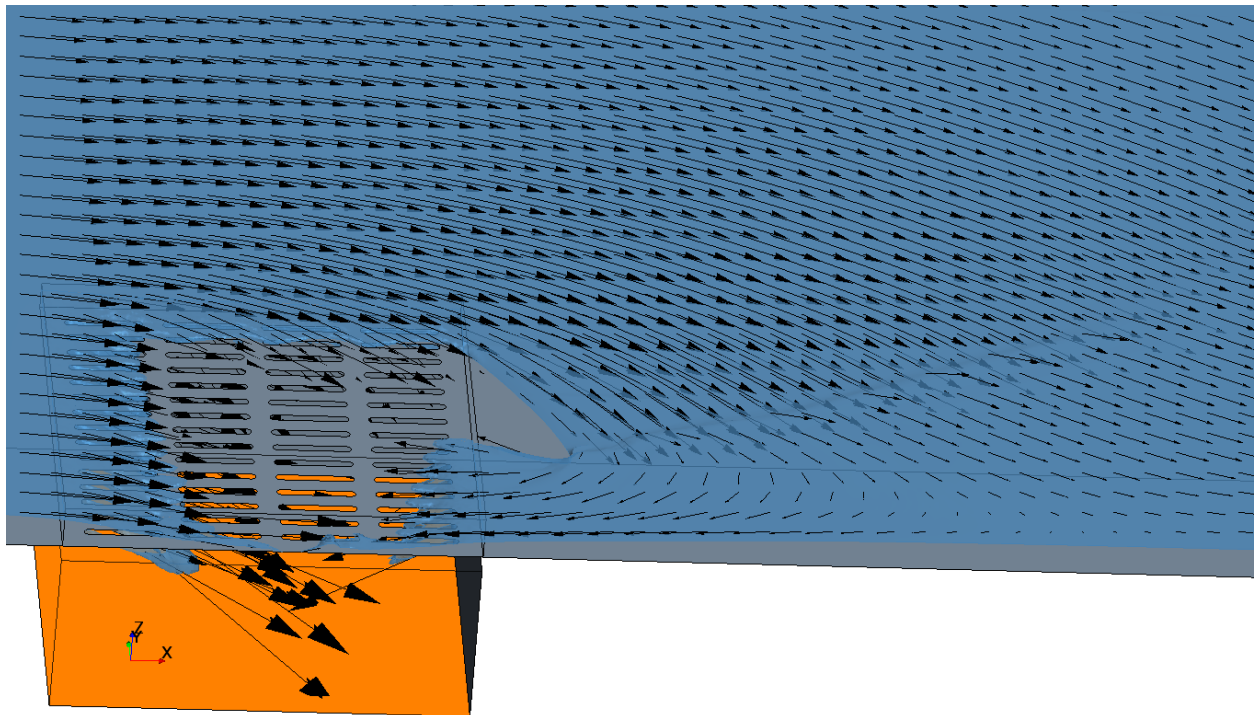


Figure 4.1 Bypass flow at curb flows back into grate for low velocity case

Views of the water surface at the grates show a major difference in flow over the two types of grates that relate to grate performance for cases with higher street longitudinal street slopes corresponding to higher volume flow rates. In ADA compliant grate case 10, the gutter and street cross slope is 0.04, the longitudinal slope is 0.05, and the volume flow of water is 17.9 cfs. In this case, the water level remains relatively high over the entire grate as shown in Figure 4.2, and only 38% of flow directly over the grate is captured, which is 14% of the total flow. Figure 4.3 shows the water surface for ADA compliant grate case 8, with same cross slopes as case 10, a longitudinal slope of 0.01, and water volume flow of 8.0 cfs. In this case, a small portion of the downstream surface of the grate is not covered by the water surface, and the grate captures about 76% of the flow directly over it with 24% of the flow directly over the grate continuing down the street.

In contrast to the ADA compliant grate cases, nearly all of the flow directly over the vane grate is captured by the grate and diverted into the catch basin. Figure 4.4 shows the water surface over the grate for the case 10.1, Table 2.1, which has the highest water volume flow, 19.6 cfs, of all cases tested and the lowest vane grate performance, 38% of total flow captured by the grate. As shown in the figure, all of the water entering from the upstream end of the grate passes through the grate into the catch basin near the mid-point of the grate. Some of the downstream street side of the vane grate is covered by water entering from the side, and some of that is not captured by the grate. However, in this lowest performing vane grate case, 97% of water passing directly over the grate is captured by the grate.

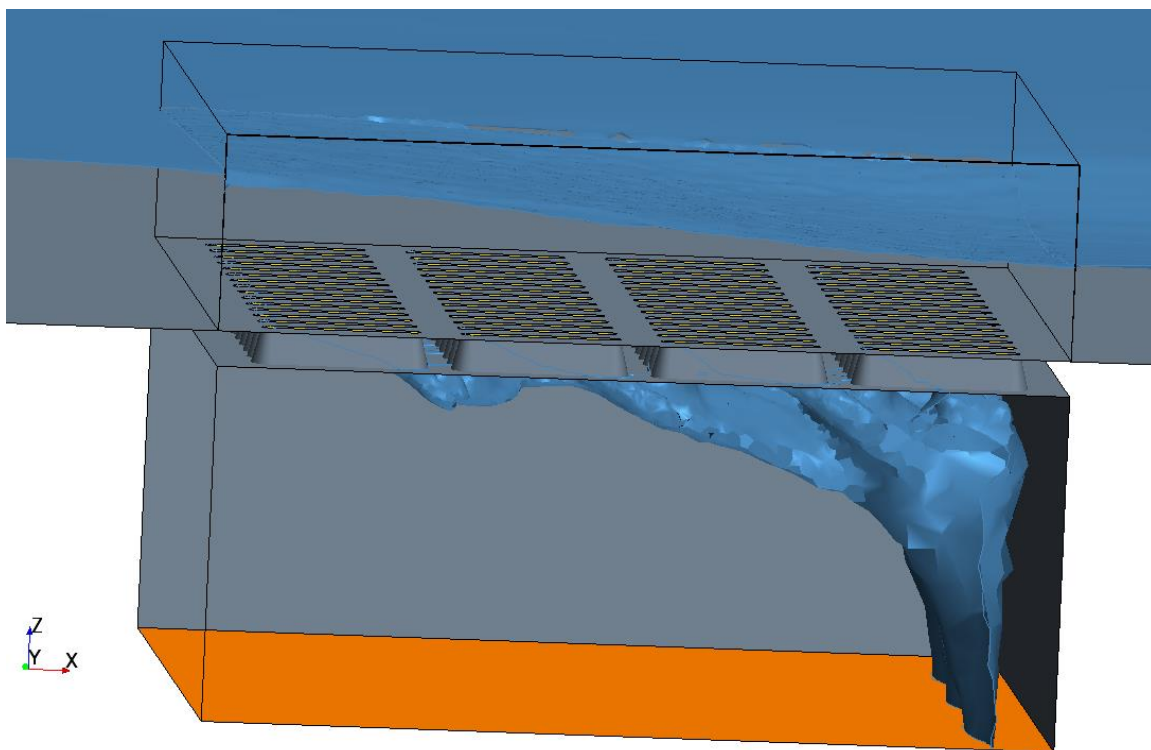


Figure 4.2 Water surface for ADA compliant grate case 10 showing relatively high water depth over the entire grate

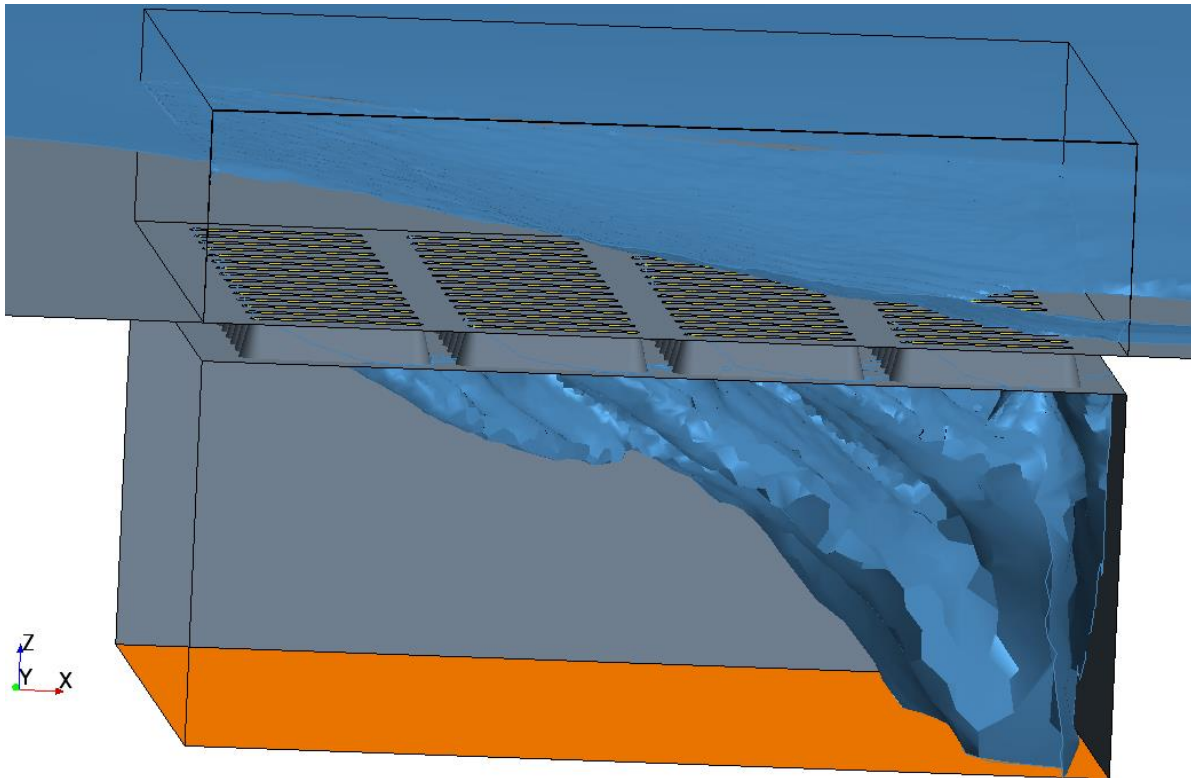


Figure 4.3 Water surface for ADA compliant grate case 8 showing only a small portion of the downstream end of the grate not covered by the water surface

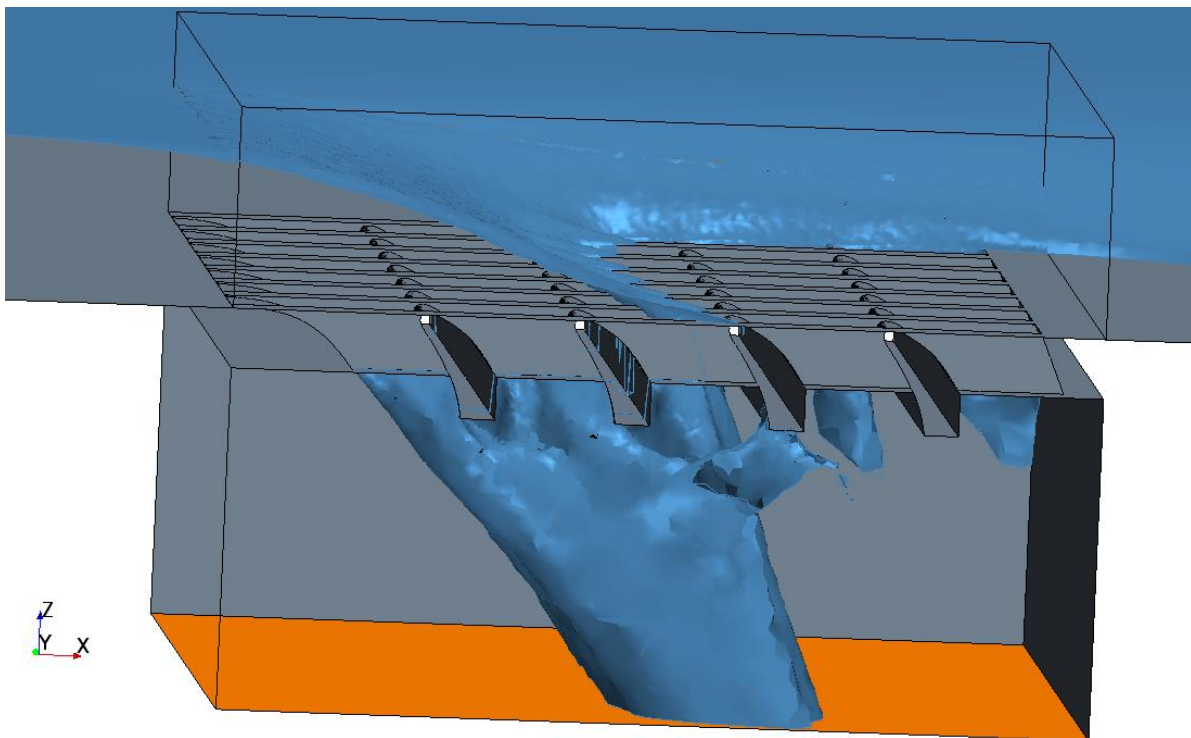


Figure 4.4 Water surface vane grate case 10.1 showing large part of downstream portion of the grate not covered by water surface

4.2 Tabulated Case Results

Table 4.1 contains the tabulated results for all cases for the ADA compliant grate. The rows of cases are divided into blocks where cases within a block may have a varying street longitudinal slope. A row label above the block lists the cross street water spread at the inlet, the gutter cross slope, and the street cross slope. The first column lists the case number. The second column lists street longitudinal slope. The third column gives the primary result of interest: the fraction of the total flow that is captured by the grate and diverted into the catch basin. The total flow rate down the street was calculated from equations in HEC 22 as described in Section 2.3. The flow rate of water through the grate into the catch basin was calculated by the CFD software as part of the solution of a case. The fraction of the total flow entering over the grate from the upstream end, from the side, and from the downstream end are listed in the next three columns. The last column lists the fraction of the flow passing over the grate that is captured by the grate.

Table 4.1 ADA compliant case results

Case	Street Longitudinal Slope (S _L)	Fraction Total Flow Captured by Grate	Fraction Total Flow over Grate Front	Fraction Total Flow over Grate Side	Fraction Total Flow over Grate Back	Fraction Flow Directly over Grate Captured
8 ft. Water Spread, 0.04 Gutter Slope, 0.04 Street Cross Slope						
1	0.003	0.6160	0.5081	0.1086	0.0000	0.9975
2	0.005	0.5410	0.4784	0.0921	0.0000	0.9510
3	0.01	0.4600	0.4671	0.0697	0.0000	0.8567
4	0.03	0.2919	0.4437	0.0325	0.0000	0.6312
5	0.05	0.2148	0.4380	0.0189	0.0000	0.4700
5.1	0.06	0.1909	0.4361	0.0159	0.0000	0.4228
10 ft. Water Spread, 0.04 Gutter Slope, 0.04 Street Cross Slope						
6	0.003	0.4908	0.4237	0.0923	0.0000	0.9535
7	0.005	0.4190	0.3957	0.0762	0.0000	0.8880
8	0.01	0.3337	0.3833	0.0567	0.0000	0.7587
9	0.03	0.1987	0.3674	0.0204	0.0000	0.5121
10	0.05	0.1442	0.3636	0.0130	0.0000	0.3829
10.1	0.06	0.1277	0.3625	0.0111	0.0000	0.3417
8 ft. Water Spread, 0.04 Gutter Slope, 0.02 Street Cross Slope						
11	0.003	0.7524	0.5829	0.1093	0.0601	1.0000
12	0.005	0.6734	0.5525	0.0926	0.0282	1.0000
13	0.01	0.5997	0.5400	0.0695	0.0000	0.9839
14	0.03	0.5176	0.5269	0.0434	0.0000	0.9076
14.1	0.04	0.4700	0.5159	0.0372	0.0000	0.8497
15	0.05	0.4281	0.5061	0.0326	0.0000	0.7947

Case	Street Longitudinal Slope (S _L)	Fraction Total Flow Captured by Grate	Fraction Total Flow over Grate Front	Fraction Total Flow over Grate Side	Fraction Total Flow over Grate Back	Fraction Flow Directly over Grate Captured
15.1	0.06	0.3915	0.4995	0.0288	0.0000	0.7411
10 ft. Water Spread, 0.02 Gutter Slope 0.04 Street Cross Slope						
16	0.01	0.3355	0.3663	0.0567	0.0000	0.7927
8 ft. Water Spread, 0.02 Gutter Slope 0.04 Street Cross Slope						
17	0.01	0.4327	0.4444	0.0701	0.0000	0.8412
8 ft. Water Spread, 0.02 Gutter Slope 0.02 Street Cross Slope						
18	0.01	0.5944	0.5660	0.0633	0.0000	0.9446
10 ft. Water Spread, 0.05 Gutter Slope 0.04 Street Cross Slope						
19	0.01	0.3407	0.3924	0.0573	0.0000	0.7577
8 ft. Water Spread, 0.05 Gutter Slope 0.04 Street Cross Slope						
20	0.01	0.4784	0.4785	0.0688	0.0000	0.8741
8 ft. Water Spread, 0.05 Gutter Slope 0.02 Street Cross Slope						
21	0.01	0.6347	0.5749	0.0683	0.0000	0.9868

Table 4.2 Vane grate case results

Case	Street Longitudinal Slope (S _L)	Fraction Total Flow Captured by Grate	Fraction Total Flow over Grate Front	Fraction Total Flow over Grate Side	Fraction Total Flow over Grate Back	Fraction over Grate Captured
8 ft. Water Spread, 0.04 Gutter Slope, 0.04 Street Cross Slope						
1	0.003	0.6867	0.5177	0.1220	0.0390	1.0000
2	0.005	0.6059	0.4811	0.1060	0.0187	1.0000
3	0.01	0.5534	0.4689	0.0873	0.0000	0.9949
4	0.03	0.4838	0.4447	0.0536	0.0000	0.9709
5	0.05	0.4665	0.4390	0.0404	0.0000	0.9731
5.1	0.06	0.4618	0.4370	0.0372	0.0000	0.9738
10 ft. Water Spread, 0.04 Gutter Slope, 0.04 Street Cross Slope						
6	0.003	0.5580	0.4270	0.1063	0.0250	0.9995

Case	Street Longitudinal Slope (S _L)	Fraction Total Flow Captured by Grate	Fraction Total Flow over Grate Front	Fraction Total Flow over Grate Side	Fraction Total Flow over Grate Back	Fraction over Grate Captured
7	0.005	0.5006	0.3988	0.0923	0.0091	1.0000
8	0.01	0.4510	0.3850	0.0737	0.0000	0.9827
9	0.03	0.3965	0.3687	0.0399	0.0000	0.9704
10	0.05	0.3866	0.3649	0.0329	0.0000	0.9719
10.1	0.06	0.3835	0.3636	0.0308	0.0000	0.9724
8 ft. Water Spread, 0.04 Gutter Slope, 0.02 Street Cross Slope						
11	0.003	0.7737	0.5854	0.1159	0.0724	1.0000
12	0.005	0.6981	0.5546	0.0999	0.0435	1.0000
13	0.01	0.6305	0.5414	0.0786	0.0103	1.0000
14	0.03	0.5713	0.5277	0.0540	0.0000	0.9821
14.1	0.04	0.5529	0.5162	0.0481	0.0000	0.9800
15	0.05	0.5387	0.5065	0.0434	0.0000	0.9795
15.1	0.06	0.5283	0.4997	0.0396	0.0000	0.9795
10 ft. Water Spread, 0.02 Gutter Slope 0.04 Street Cross Slope						
16	0.01	0.4332	0.3680	0.0742	0.0000	0.9798
8 ft. Water Spread, 0.02 Gutter Slope 0.04 Street Cross Slope						
17	0.01	0.5296	0.4460	0.0894	0.0000	0.9892
8 ft. Water Spread, 0.02 Gutter Slope 0.02 Street Cross Slope						
18	0.01	0.6289	0.5664	0.0756	0.0000	0.9797
10 ft. Water Spread, 0.05 Gutter Slope 0.04 Street Cross Slope						
19	0.01	0.4585	0.3943	0.0738	0.0135	0.9793
8 ft. Water Spread, 0.05 Gutter Slope 0.04 Street Cross Slope						
20	0.01	0.5636	0.4803	0.0855	0.0000	0.9960
8 ft. Water Spread, 0.05 Gutter Slope 0.02 Street Cross Slope						
21	0.01	0.6658	0.5758	0.0764	0.0000	1.0000

4.3 Effects of Increasing Longitudinal Street Slope

Three sets of cases had fixed upstream water spread, gutter cross slope, and street cross slope with increasing street longitudinal slope, varying from 0.003 to 0.06. For these cases, the flow boundary variable that changes with the increasing street slope is the volume flow rate or equivalently the

mean velocity at the domain (upstream) inlet, which increases with the increasing slope. As detailed previously in Section 2.3, the volume flow was calculated based on the geometry and water spread using formulas from HEC 22 [2]. As the volume of flow increases, a decline in performance of the grates is expected. Figure 4.5 and Figure 4.6, show plots of this expected trend for the ADA compliant and vane grates respectively. The ordinate is the fraction of the total flow that is diverted by the grate into the catch basin, and the abscissa is the longitudinal street slope. The captured fraction drops rapidly then more slowly with increasing longitudinal street slope. The highest performance in terms of captured fraction is at the lowest street slope of 0.003, ranging from 0.49 to 0.75 for the ADA compliant grate and from 0.56 to 0.77 for the vane grate, a nearly equal performance range for the three sets of cross street parameters. The lowest performance in terms of captured fraction is at the highest street slope of 0.06, ranging from 0.13 to 0.39 for the ADA compliant grate and from 0.38 to 0.53 for the vane grate. The amount of drop off in performance of the vane grate with increasing longitudinal street slope is significantly less than that for the ADA grate.

The plots in Figure 4.7 to Figure 4.9 compare the performance of the ADA compliant grate against the vane grate directly for the three sets of cross street parameters. The ordinate is the fraction of the total flow that is diverted by the grate into the catch basin, and the abscissa is the longitudinal street slope. Figure 4.7 compares the performance of the ADA and vane grate for cases with an 8 foot water spread across gutter and street with gutter and cross street slopes equal to 0.04. At the smallest longitudinal street slope of 0.003 the ADA compliant grate captures 62% of the flow while the vane grate captures 69%. At this low longitudinal street slope, the ADA grate captures about 10% less water than the vane grate. As the longitudinal street slope increases the performance of both grates drops off, and the ADA grate performance drops off much faster. At the highest longitudinal street slope of 0.06, the ADA grate captures only 19% of the flow while the vane grate captures 46%. At this highest street slope tested, the vane grate is still capturing about half of the flow and about 2.4 times the amount captured by the ADA compliant grate. The situation is worse for a greater water spread width of 10 feet as shown in Figure 4.8. At a longitudinal street slope of 0.003 the performance difference between the grates is about the same; the vane grate captures about 10% more of the flow. At the maximum longitudinal slope tested of 0.06, the vane grate captures 3 times the amount captured by the ADA compliant grate. The amount captured by the ADA grate has dropped to about 13% of the flow.

In the third set of varying longitudinal street slope cases, the cross street slope is reduced by half from 0.04 to 0.02. With the cross street water spread fixed, this change significantly lowers the water depth at the curb yielding a much shallower flow approaching the grates. The ADA compliant grate performance is still below the vane grate with the gap increasing as the longitudinal street slope increases as shown in Figure 4.9, but the performance gap is not nearly as large as for the sets of cases with cross street slope of 0.04. For these cases, the ADA compliant and vane grate performance is nearly the same with 75% of flow captured by the ADA grate and 77% of flow captured by the vane grate. At the highest street slope tested, 0.06, the vane grate captures 35% more of the flow than the ADA grate.

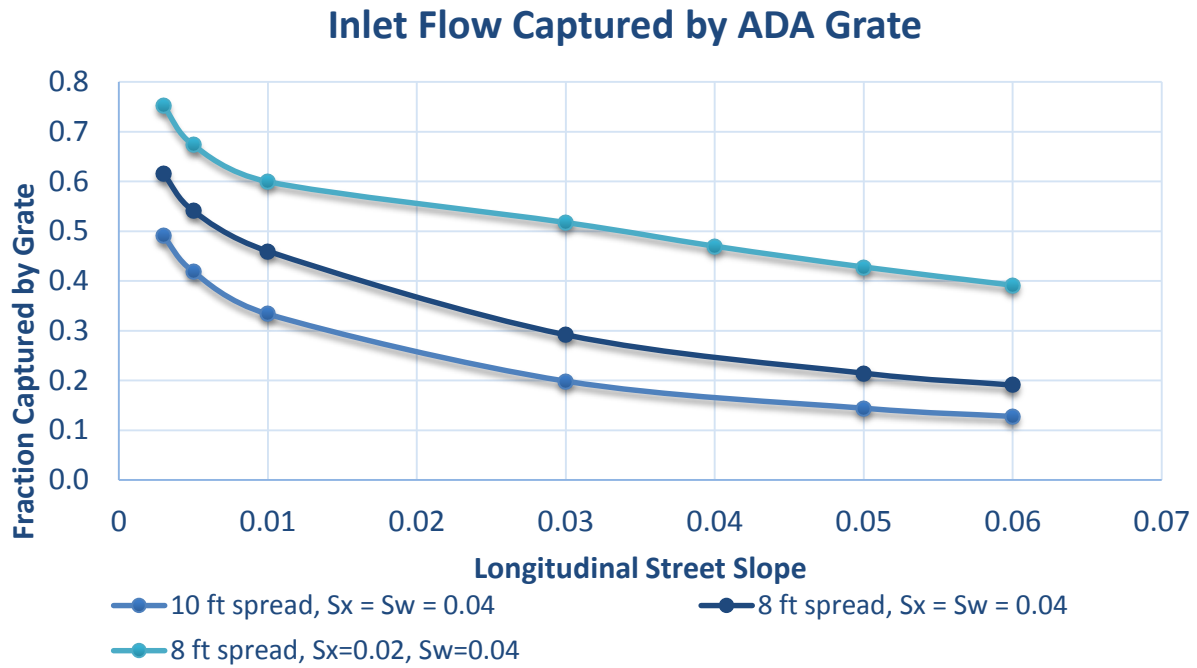


Figure 4.5 Fraction of total flow captured by ADA compliant grate for three sets of cross street conditions

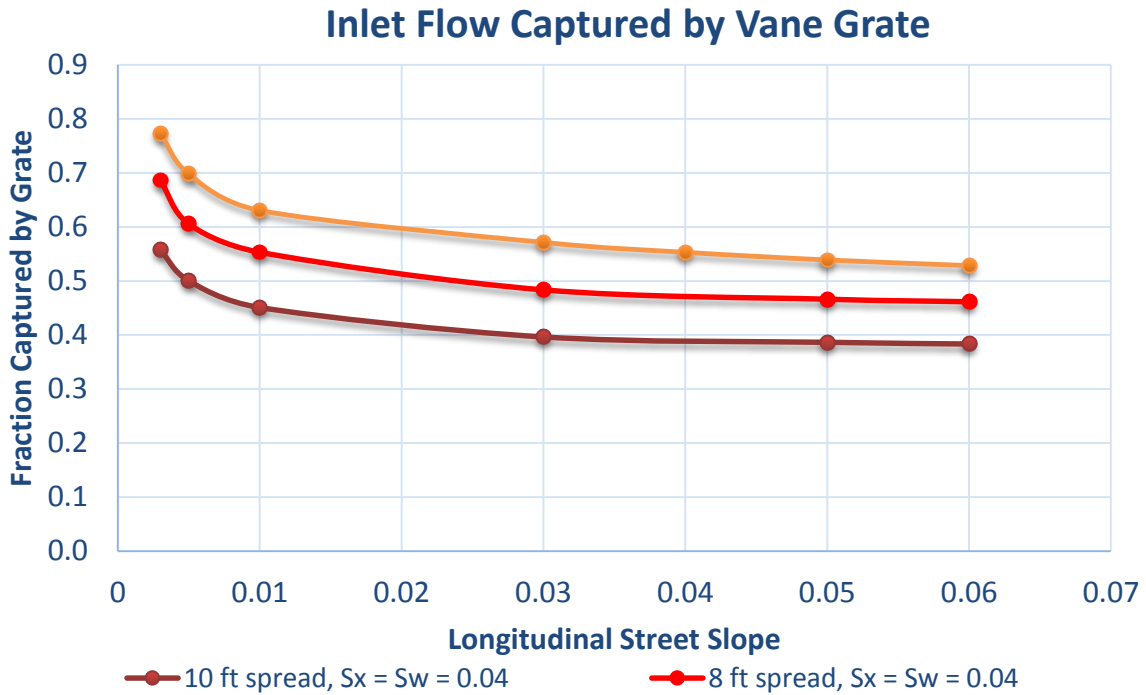


Figure 4.6 Fraction of total flow captured by vane grate for three sets of cross street conditions

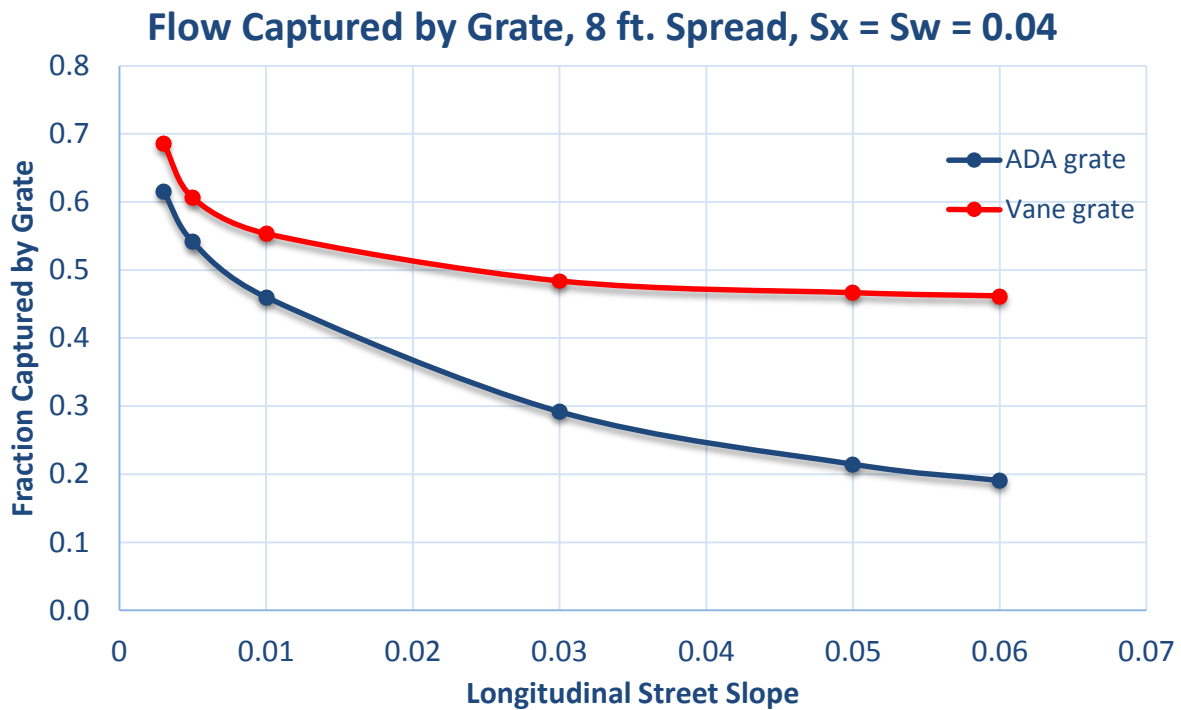


Figure 4.7 Comparison for flow captured by ADA and vane grate showing more rapid drop off in performance of ADA grate as longitudinal street slope increases with 8 ft. spread

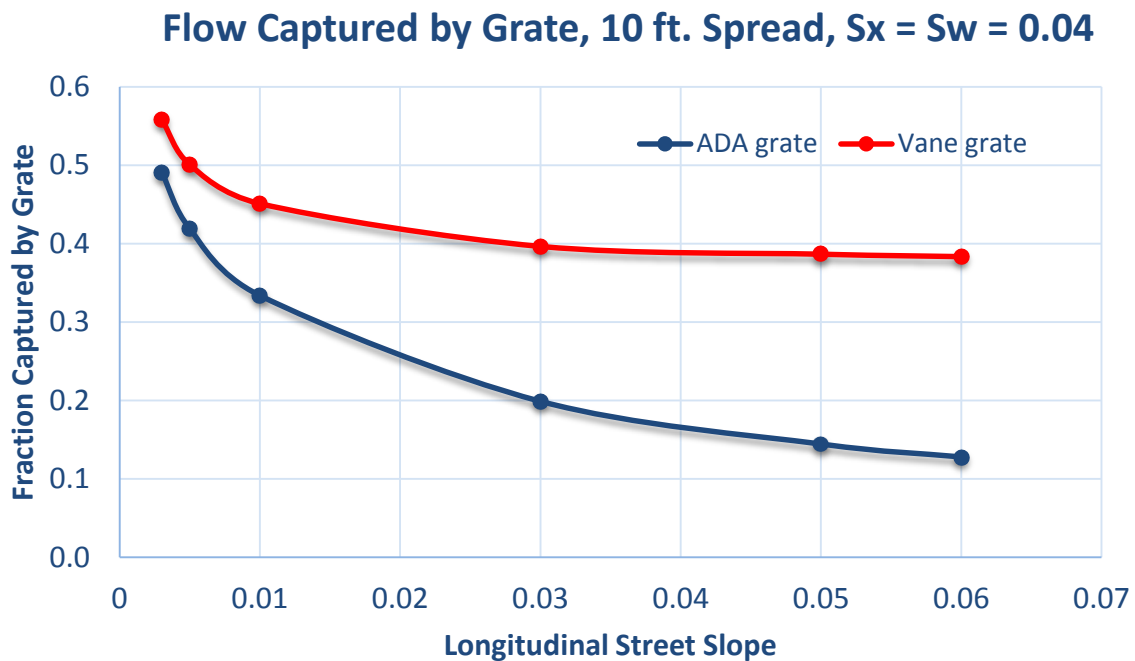


Figure 4.8 Comparison for flow captured by ADA and vane grate showing more rapid drop off in performance of ADA grate as longitudinal street slope increases with 10 ft. spread

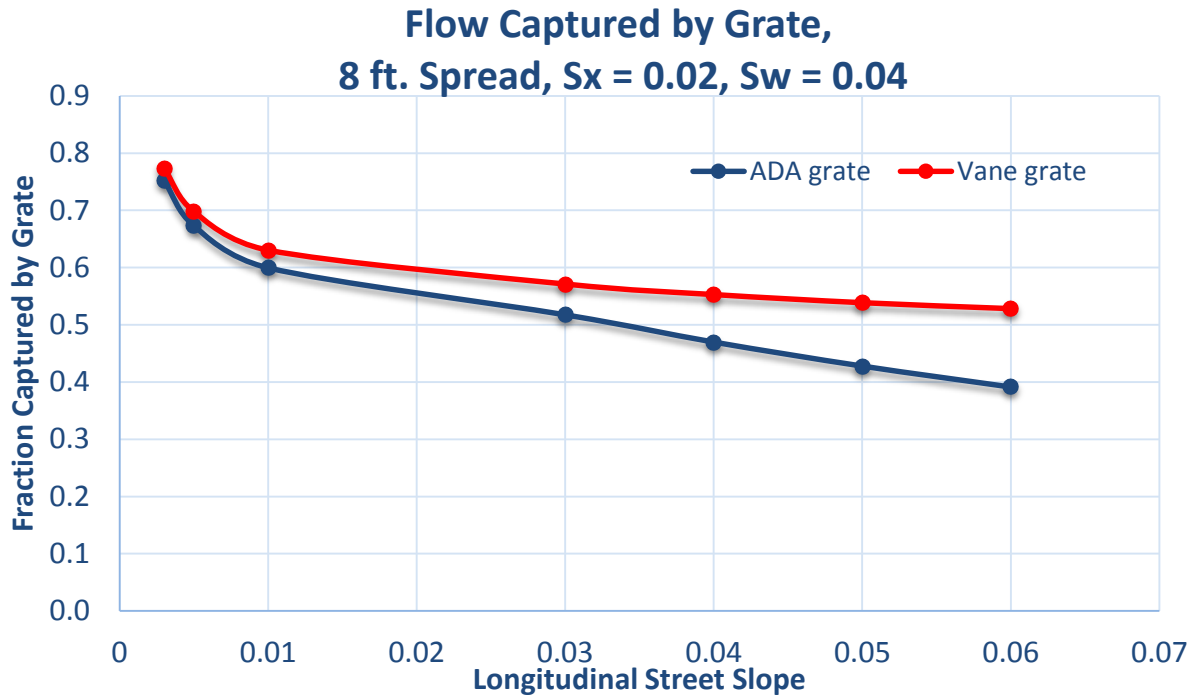


Figure 4.9 Comparison for flow captured by ADA and vane grate showing more rapid drop off in performance of ADA grate as longitudinal street slope increases with 8 ft. spread and 0.02 street cross slope

The plots in Figure 4.10 to Figure 4.12 compare the amount of water entering over the ADA compliant and vane grates from the side for the three sets of cross street parameters where the longitudinal street slope was varied in the CFD analysis. The ordinate is the fraction of the total flow moving over a grate from the side. The abscissa is the longitudinal street slope. The fraction of flow entering over the grates from the sides is at a maximum at the lowest longitudinal street slope of 0.003. At that slope, it ranges from 10.6% to 12.2% for the vane grate and from 9.2% to 10.9% for the ADA compliant grate.

For all cases the fraction of water entering over the grates from the side decreases as the longitudinal street slope increases and is less for the ADA compliant grate than the vane grate. The fraction of flow over the grates from the sides also drops off faster for the ADA compliant grate than for the vane grate. At the highest longitudinal street slope of 0.06, the flow entering over the side drops to about 4% of the total flow for the sets of cases with 8 foot upstream water spread and to about 3% for the case with 10 foot water spread. For the longitudinal slope of 0.06, the fraction of flow entering over the ADA grate from the side is 1.6% for the 8 foot water spread with gutter and street cross slope of 0.04, 1.1% for the 10 foot water spread with gutter and street cross slope of 0.04, and 2.95 for the 8 foot water spread with 0.04 gutter slope and 0.02 street slope.

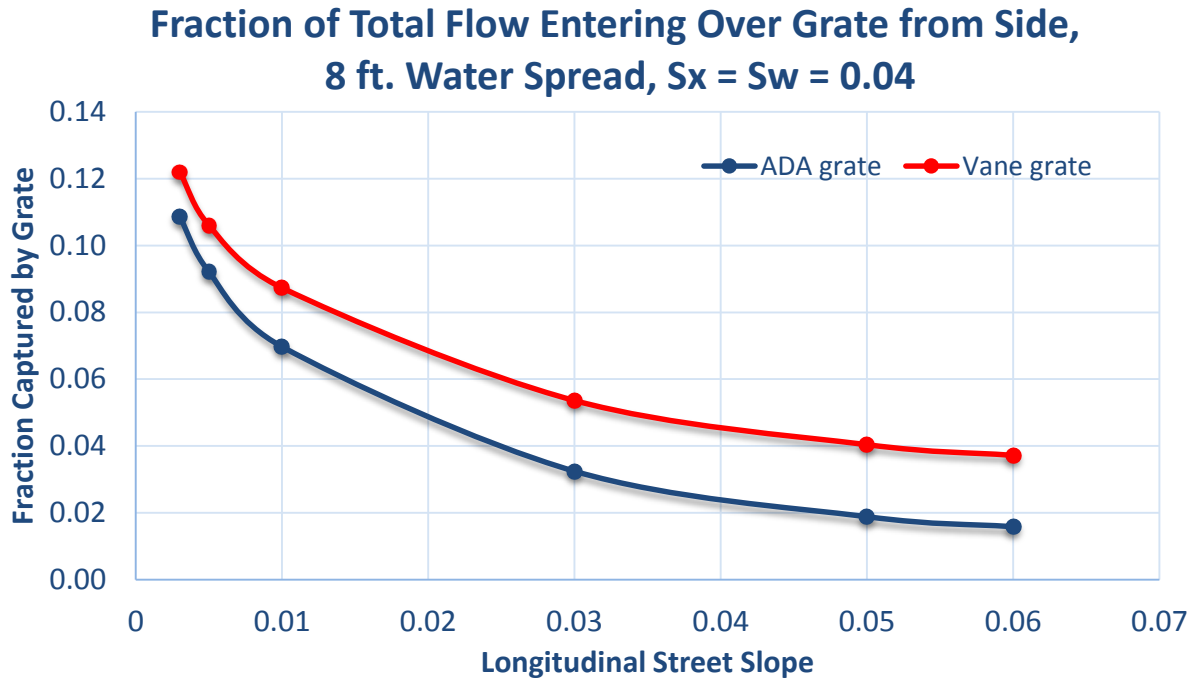


Figure 4.10 Comparison of flow entering over ADA and vane grate from side showing more rapid drop off in performance of ADA grate with 8 ft. spread

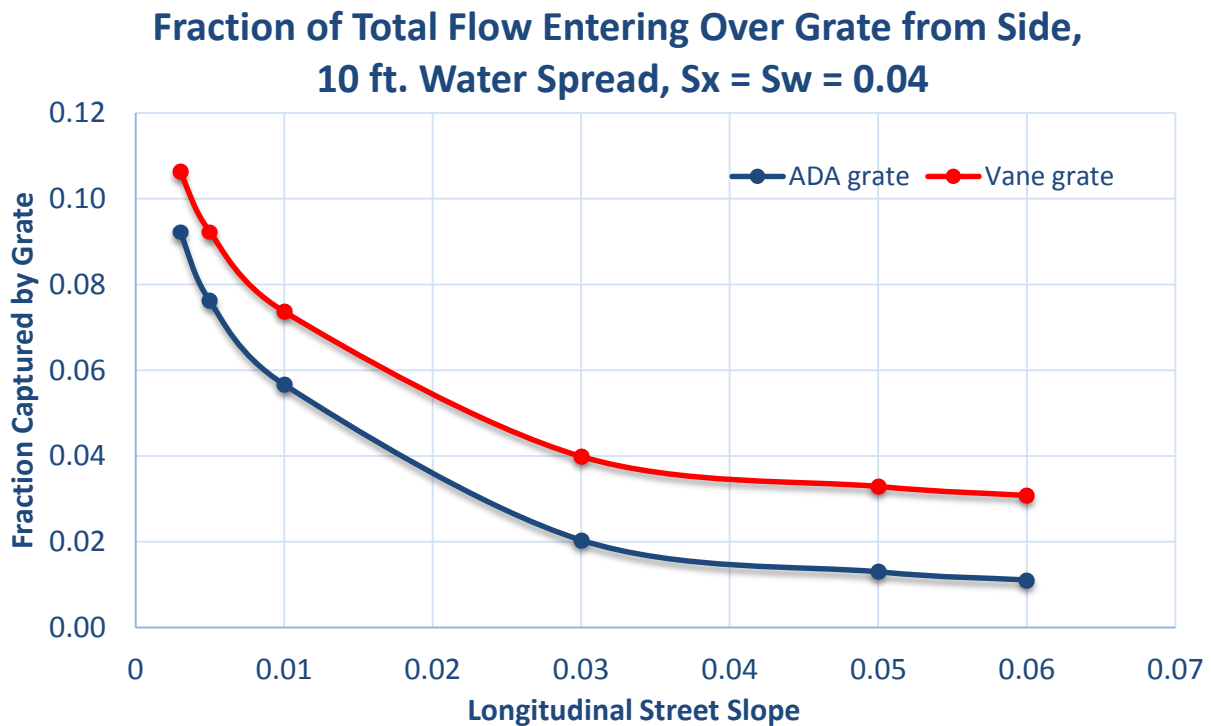


Figure 4.11 Comparison of flow entering over ADA and vane grate from side showing more rapid drop off in performance of ADA grate with 10 ft. spread

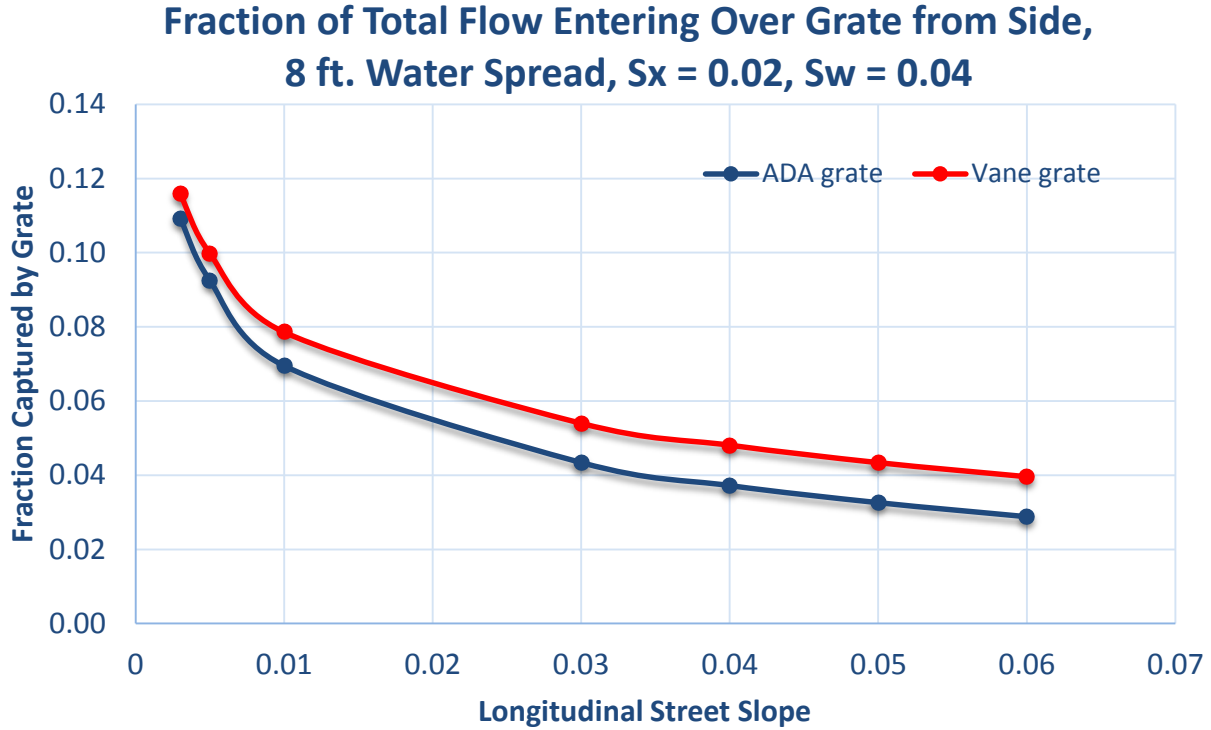


Figure 4.12 Comparison of flow entering over ADA and vane grate from side showing more rapid drop off in performance of ADA grate with 8 ft. spread and 0.02 gutter cross slope

4.4 Correlation of All Case Results with Upstream Reynolds Number and Froude Number at Curb

Data curve fitting was done including conditions and results from all of the cases using the capabilities in MS Excel to fit functions to the result data. The best fits were obtained with log functions for fraction of flow captured by the grates and fraction of total flow entering over the grates from the side. The best fit for fraction of flow moving directly over a grate that is captured was obtained using a linear fit.

The upstream Reynolds number is defined by:

$$R_e = \frac{\rho V d_h}{\mu} = \frac{4\rho Q}{(P_w + P_s + h)\mu} \quad 4.1$$

where ρ is the water density, V is the mean velocity at the inlet cross section, d_h is the hydraulic diameter at the inlet, μ is the water viscosity, Q is the volume flow rate at the inlet, P_w is the gutter width, P_s is the wetted street width, and h is the water depth at the curb. The hydraulic diameter at the inlet is calculated as four times the flow cross section area divided by the wetted perimeter:

$$d_h = \frac{4A}{(P_w + P_s + h)} \quad 4.2$$

where A is the inlet cross section area and $Q = VA$.

The upstream Froude number at the curb is calculated as:

$$F_r = \frac{V}{\sqrt{gh}} \quad 4.3$$

Where g is the gravity acceleration.

The fraction of flow captured by a grate was plotted against upstream inlet velocity, Reynolds number, and Froude number, and curves were fitted to the data. The best curve fit was obtained from the plot of fraction of flow captured against Reynolds number, and the upstream Froude number at the curb did not correlate well with the fraction captured, as shown in Figure 4.13.

The upstream Reynolds number at the domain inlet represents a ratio of flow inertia to the viscous resistance of the flow by the street and curb surfaces. The graph in Figure 4.13 shows that as the Reynolds number increases, the captured fraction of the flow decreases for both of the grates. However, it decreases significantly more for the ADA compliant grate. From Reynolds number 44,000 to 790,000 the fraction of flow captured by the vane grate drops from 0.77 to 0.38, a factor of two, while the ADA compliant grate drops from 0.75 (nearly the same as the vane grate) to 0.13 at $R_e = 790,000$, a decrease by a factor of 5.6.

For the vane grate the fraction of total flow captured, C_f , as a function of upstream Reynolds number is:

$$C_f = -0.125 \ln R_e + 2.069 \quad 4.4$$

with a coefficient of determination of 0.90, and the function for the ADA compliant grate is:

$$C_f = -0.215 \ln R_e + 3.0613 \quad 4.5$$

with a coefficient of determination of 0.96.

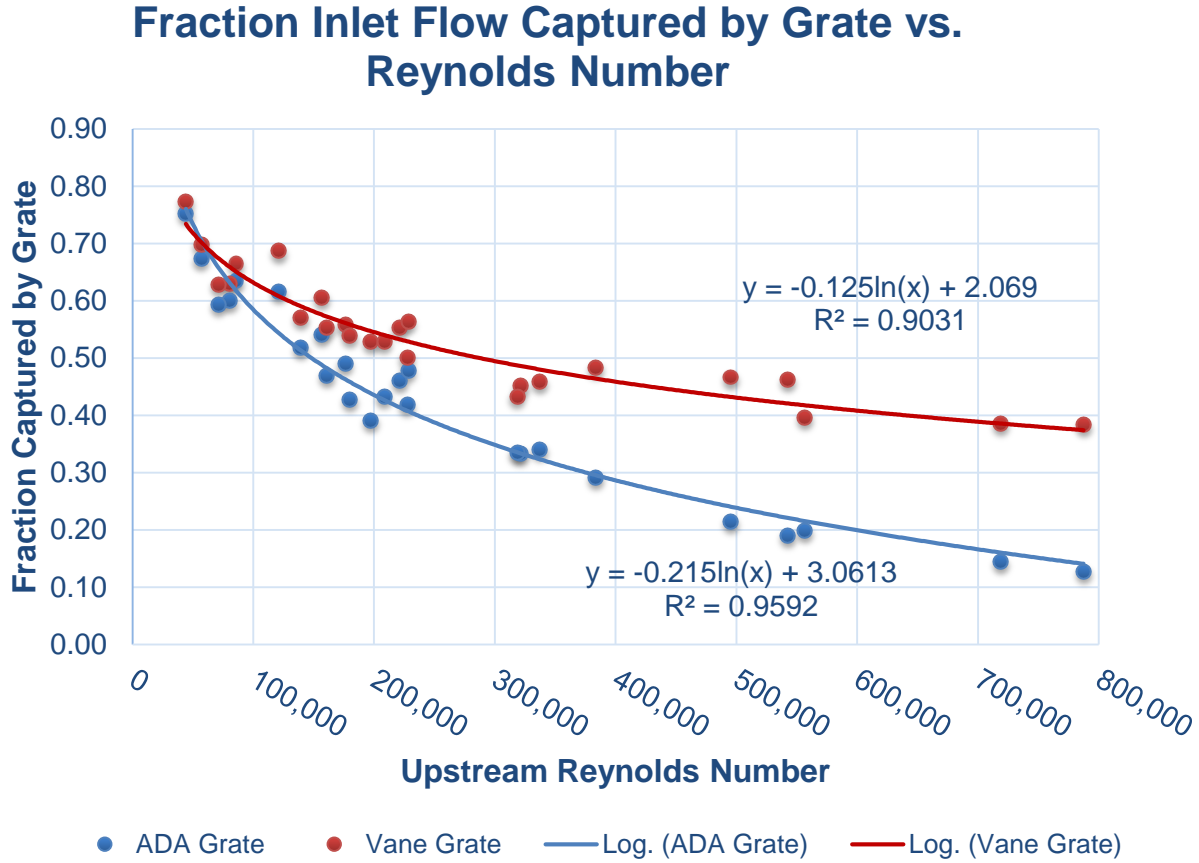


Figure 4.13 Fraction of flow captured by grates correlated with upstream Reynolds number

Figure 4.14 shows a plot of the total flow coming from the upstream that crosses over the grate from the side versus the upstream Froude number at the curb. The flow from the side correlated well with curb Froude number, but not Reynolds number. Flow entering over the grates from the side is relatively low for all cases and is lower by an increasing percentage as the Froude number at the curb increases. At a curb Froude number of 0.5 about 12% of the incoming flow enters over the vane grate from the side while about 11% of the flow with the ADA grate comes from the side. At curb Froude number 2.7 only 3% of the flow enters over the vane from the side and the amount drops to 1% of flow from the side for the ADA grate.

For the vane grate the fraction of flow entering over the grate from the side, S_f , as a function of upstream Reynolds number is:

$$S_f = -0.052 \ln F_r + 0.0823 \quad 4.6$$

with a coefficient of determination of 0.95, and the function for the ADA compliant grate is:

$$S_f = -0.057 \ln F_r + 0.0685 \quad 4.7$$

with a coefficient of determination of 0.97.

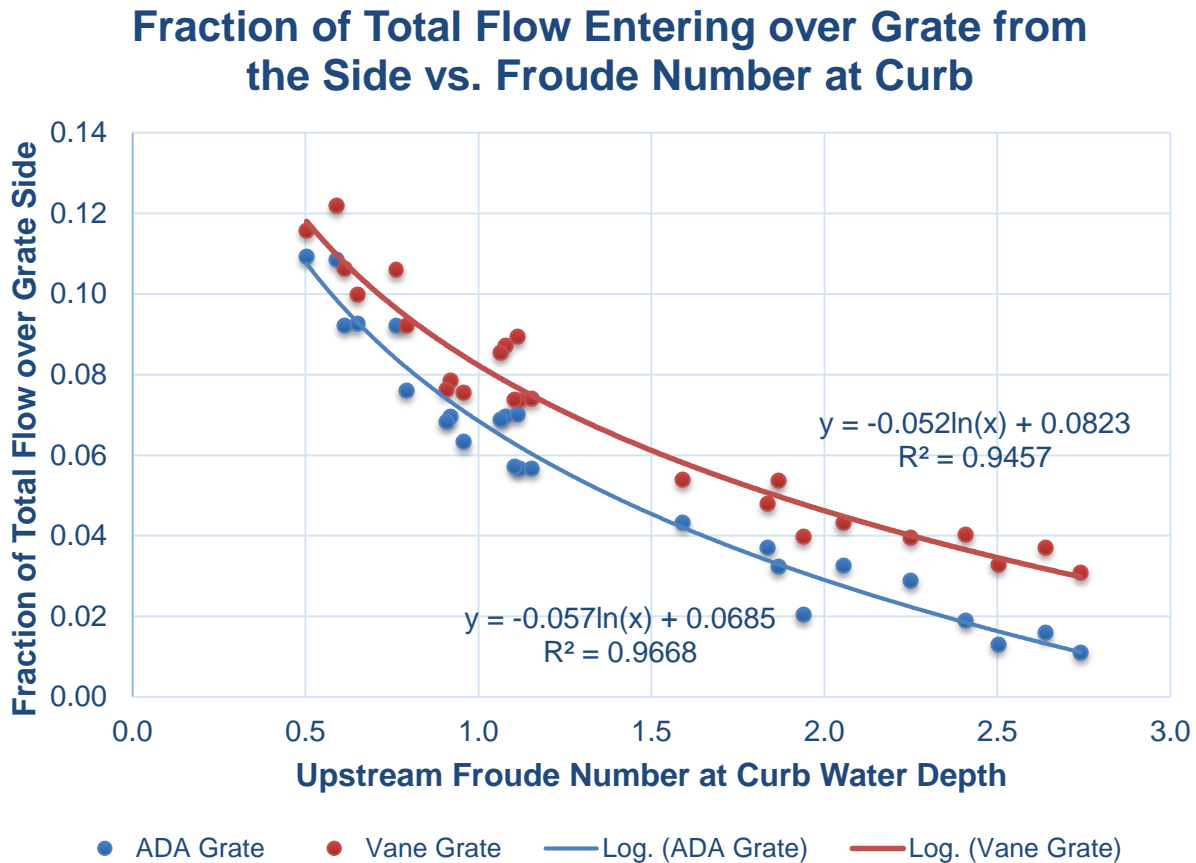


Figure 4.14 Fraction of flow over grate from the side correlated with upstream Froude number at the curb water depth

A good picture of the difference in hydraulic performance between the two grates is apparent in Figure 4.15. The fraction of flow going directly over the grate that is captured by the grate is plotted against the upstream Reynolds number. For the vane grate once water moves over the grate from the upstream edge, side, or back flow from downstream in a few cases, very little of the flow directly over the vane grate crosses without flowing down into the catch basin for all cases regardless of the Reynolds number. There is a small increase in the amount of water directly over the grate that is not captured with increasing Reynolds number, but at most it is less than 3%.

The plot also shows very different performance with the ADA compliant grate. As the upstream Reynolds number increases resulting from more water inertia and/or less street and curb surface resistance, the amount of flow passing directly over the ADA grate that is captured by the grate drops steadily from conditions at Reynolds number around 80,000 where nearly all of it is captured to Reynolds number 790,000 where only about 34% of water passing directly over the ADA grate is captured.

For the vane grate the fraction of flow directly over the grate that is captured, D_f , as a function of upstream Reynolds number is:

$$D_f = -4 \times 10^{-8} \ln R_e + 0.9974 \quad 4.8$$

with a coefficient of determination of 0.53. This low coefficient of determination is a consequence of the fraction of flow passing directly that is captured being nearly constant and only weakly dependent on the Reynolds number. The function for the ADA compliant grate is:

$$D_f = -1 \times 10^{-6} \ln R_e + 1.0531 \quad 4.9$$

with a coefficient of determination of 0.93.

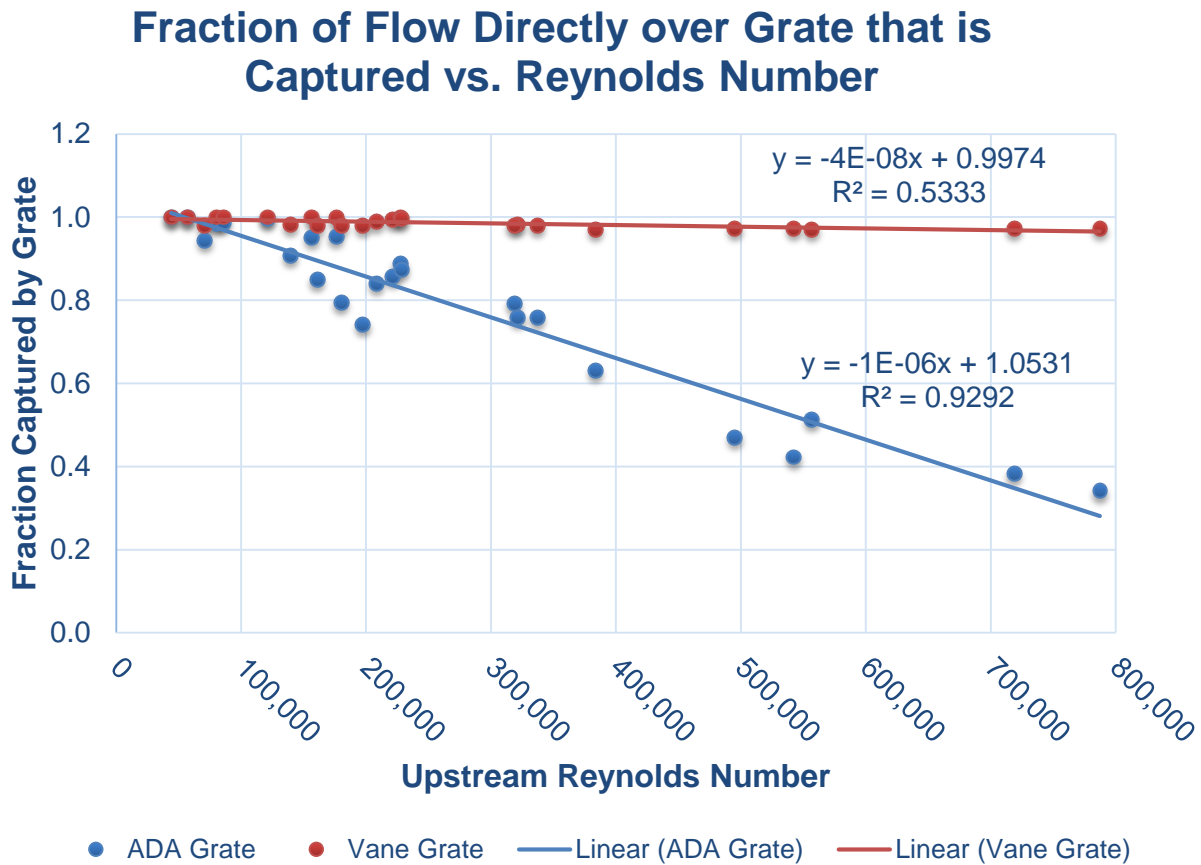


Figure 4.15 Fraction of flow directly over that grate that is captured by the grate correlated with upstream Reynolds number

Chapter 5

Summary and Conclusions

The hydraulic performance of an ADA compliant grate geometry, R-3210-Q from the Neenah grate catalog, was determined with a full scale three dimensional model of the grate in the street using CFD software for a parametric matrix of street geometry parameters and water spreads. The analysis was repeated using a vane grate model based on the R-3210-L grate in the Neenah grate catalog. The two phase volume of fluid (VOF) model for modeling free surface flows was used in the CFD software. The computational domain was divided into three regions to allow generation of near optimum computational meshes in each region. The regions were: (1) a 20 foot long by 10 foot wide section of street with water and air above it, (2) the volume immediately above the grate, and (3) the grate and catch basin section cut at about 1.5 feet below the street level. A parametric set of test cases was specified by MnDOT. These included street geometry with 0.04 gutter cross slope, 0.02 and 0.04 street cross slopes for six street longitudinal slopes ranging from 0.003 to 0.06. A few additional cases with varied gutter cross slopes were run with a street longitudinal slope of 0.01. Water spreads across the street were 8 and 10 feet including a 2 foot gutter width.

The ADA compliant grate has a large number of much narrower slots than those used in the common street drain grates, and therefore its hydraulic performance was expected to be below that of the vane grate. As expected, the performance of the ADA compliant grate was lower than that of the vane grate in each of the test cases. As the volume flow rate is reduced below those of the test cases, there is a volume flow low enough, which was not determined, where the ADA grate would capture all of the flow making the performance of the two grates equal for conditions with volume flows less than that amount. The lowest volume flow rate tested was 0.867 cfs with a gutter cross slope of 0.04, a street cross slope of 0.02, an 8 foot water spread, and street longitudinal slope of 0.003. For these conditions, the performance of the ADA compliant and vane grate were very close, within 3% of each other, with the vane grate capturing 77% of the total flow and the ADA compliant grate capturing 75%. The largest difference in performance occurred at the highest volume flow rate of 19.6 cfs with a gutter and street cross slope of 0.04, a 10 foot water spread, and a longitudinal slope of 0.06. For these conditions, the vane grate performance was three times that of the ADA compliant grate. The vane grate captured 38% of the total flow while the ADA compliant grate captured only 13%.

Three sets of cases were tested where only the longitudinal street slope parameter was varied from 0.003 to 0.06. In these case sets the water volume flow rate and mean velocity increases with increasing longitudinal street slope. For these case sets, the performance of the two grate types was relatively close at the lowest longitudinal street slope and corresponding low volume flow rate. In the worst case set, the ADA compliant grate performance was about 12% below that of the vane grate. As the longitudinal street slope was increased, the performance of both grates decreased, but the performance of the ADA compliant grate decreased much faster

than the vane grate, yielding in the worst case, a vane grate hydraulic performance that was 3 times the ADA compliant grate performance.

Single parameter correlations were sought to characterize the relation between the various parameters and grate performance quantified as the fraction of total flow captured by the grate. Relations were also sought for the fraction of total flow entering over the grate from the side of the grate and the fraction of the flow directly over the grate that is captured by the grate. The upstream Reynolds number, defined in terms of the water volume flow rate and curb and street wetted perimeter was found to be the best parameter to correlate with the fraction of total flow captured by the grates and with the fraction of flow directly over the grate that is captured by the grate. The upstream Reynolds number represents a ratio of flow inertia to the viscous resistance of the flow by the street and curb surfaces. The relation between Reynolds number and grate performance was found to be best fit for all cases by a logarithmic decay function of the form $C_f = -A \ln(R_e) + B$, where A and B are fitting constants and C_f is the fraction of flow captured by the grate. The coefficient of determination of these relations was 0.90 for the vane grate cases and 0.94 for the ADA compliant grate cases, indicating a very high degree of correlation between upstream Reynolds number and grate performance under varying street geometry and flow conditions. For the ADA compliant grate, that pre-logarithm constant was 0.215, nearly twice that for the vane grate with $A = 0.125$. For upstream Reynolds numbers less than about 120,000 the flow captured by the grates is comparable, with the ADA compliant grate capturing 90% or more of the flow fraction captured by the vane grate. However, as Reynolds number increases, the performance of the ADA grate drops logarithmically. At Reynolds number 200,000 the ADA grate performance is about 25% lower than the vane grate and at 600,000 the ADA compliant grate captures half the flow captured by the vane grate.

The major factor leading to the hydraulic performance difference between the two grates appears to be the fraction of flow directly over the grates that is captured by the grates. The difference is clearly seen when this quantity is plotted against upstream Reynolds number. Nearly all of the flow entering into the space directly above the vane grate is captured and diverted into the catch basin. A drop off of only 3% occurs from Reynolds number 50,000 to 800,000. For the ADA compliant grate, the fraction of flow directly over the grate drops linearly from 100% at Reynolds number 50,000 to only 34% at a Reynolds number of about 790,000.

References

- [1] Neenah Foundry, 15th Edition Catalog, Neenah Construction Castings, Neenah, Wisconsin.
- [2] Hydraulic Engineering Circular No. 22, Third Edition, Urban Drainage Design Manual, FHWA-HHI-10-009, Federal Highway Administration, September 2009.
- [3] Hubert Chanson, The Hydraulics of Open Channel Flow: An Introduction, 2nd Edition, Elsevier, 2004, p. 72.
- [4] C. McGahey ,P. G. Samuels. (2004) River roughness – the integration of diverse knowledge. Proceedings of the 2nd International Conference on Fluvial Hydraulics River Flow, 405 – 414.



Energy Systems Division
Argonne National Laboratory
9700 South Cass Avenue, Bldg. 362
Argonne, IL 60439-4815

www.anl.gov



Argonne National Laboratory is a U.S. Department of Energy
laboratory managed by UChicago Argonne, LLC